

**FRACTURE TOUGHNESS OF CONVENTIONAL, MILLED AND PRINTED
DENTURE BASES**

by

Ravdeep Singh Mann

A THESIS SUBMITTED IN PARTIAL FULFILLMENT OF
THE REQUIREMENTS FOR THE DEGREE OF
MASTER OF SCIENCE

in

THE FACULTY OF GRADUATE AND POSTDOCTORAL STUDIES
(Craniofacial Science)

THE UNIVERSITY OF BRITISH COLUMBIA
(Vancouver)

January 2022

© Ravdeep Singh Mann, 2022

The following individuals certify that they have read, and recommend to the Faculty of Graduate and Postdoctoral Studies for acceptance, a thesis entitled:

Fracture toughness of Conventional, Milled and Printed denture bases

submitted by Ravdeep Singh Mann in partial fulfillment of the requirements for
the degree of Master of Science
in Craniofacial Science

Examining Committee:

Dr. N. Dorin Ruse, Professor, Department of Oral Biological & Medical Sciences, UBC

Supervisor

Dr. Nesrine Mostafa, Assistant Professor, Department of Oral Health Sciences, UBC

Supervisory Committee Member

Dr. Tom Troczynski, Professor, Department of Materials Engineering, UBC

Supervisory Committee Member

Dr. Chris Wyatt, Professor, Department of Oral Health Sciences, UBC

Additional Examiner

Abstract

Purpose: The aim of this study was to determine K_{IC} of a conventional denture base material, using the notchless triangular prism (NTP) specimen K_{IC} test, and compare it with that of CAD/CAM and 3D-printed denture base materials after 7 d and 90 d storage in 37 °C water.

Materials and methods: Lucitone 199 (C), Lucitone 199 CAD (M) and Lucitone Digital Print (P) (Dentsply International Inc., York, PA) were used to fabricate NTP specimens (40/group). Samples were stored in 37 °C water for 7 d (20/group) and 90 d (20/group) and were conditioned, according to ISO 20795-1. For testing, samples were secured in custom-made jigs, replicating the chevron-notch short rod specimen configuration. The test assembly was loaded in tension (0.1 mm/min) until crack arrest or failure. The maximum-recorded load was used to calculate K_{IC} . Two-way ANOVA, followed by Scheffé multiple mean comparisons ($\alpha = 0.05$), independent t-tests and Weibull statistics were used to analyze the results. Light and scanning electron microscopy were used to characterize fractured surfaces.

Results: Crack arrest was observed in all test specimens. The analyses of the results have shown that the three tested materials had significantly different K_{IC} at 7 d and 90 d, with the same ranking, i.e., $P > C > M$ ($p < 0.005$).

The analyses of the results have also shown that ageing in 37 °C water for 90 d resulted in a significant decrease in K_{IC} in the C and M groups ($p < 0.001$).

Significant crazing was observed in the 3D-printed specimens, which resulted in them having significantly larger work of fracture values ($\sim 8 \text{ KJ/m}^2$ vs $\sim 3 \text{ KJ/m}^2$).

Conclusion: The tested 3D-printed denture base material had significantly higher K_{IC} , exhibited crazing, had a higher absorbed energy before fracture and was stable under ageing conditions, suggesting that it could be more resistant to crack propagation than the tested conventional and milled materials. The tested milled denture base showed the least resistance to crack propagation, with the lowest K_{IC} values both at 7 d and 90 d. Water storage for 90 d significantly decreased K_{IC} of the tested conventional and milled materials.

Lay Summary

The ease and efficiency afforded by CAD/CAM technology in other fields of dentistry has led to its adoption in the manufacturing of removable prostheses. The most commonly used removable prostheses are denture bases. The technology shift and its application in manufacturing of denture bases has led to development of novel denture base materials. These materials are being commercialized as having better mechanical and physical properties, along with improved biocompatibility. However, the available evidence and independent assessment of these materials is lacking. The long-term behavior of the properties of these materials has also not been assessed. To help clinicians in their selection of a suitable denture base material, the aim of the study was to assess the short and long-term ability of three different denture base materials to resist crack propagation.

Preface

All components of this project, including research, sample calculations, sample preparation and testing, statistical analysis, and dissertation writing, were completed by Ravdeep Singh Mann without collaboration, under the guidance and expertise of my supervisor, Dr. N. Dorin Ruse, UBC Faculty of Dentistry. Dr. Nesrine Mostafa, UBC Faculty of Dentistry and Dr. Tom Troczynski, UBC Department of Materials Engineering were part of the supervisory research committee. This was an in-vitro study with involvement of no human or animal subjects, and no biohazardous materials, hence no Ethics Board approval was required.

Table of Contents

Abstract	iii
Lay Summary.....	v
Preface	vi
List of Tables.....	xi
List of Figures	xii
List of Equations.....	xiv
List of Abbreviations	xv
List of Symbols.....	xvii
Acknowledgements	xviii
Dedication.....	xix
Chapter 1: Introduction.....	1
1.1 History of Denture Bases.....	2
1.2 Classification of Denture Bases.....	3
1.3 Poly(Methyl Methacrylate) as Denture Base Material	5
1.3.1 Poly(methyl methacrylate)	5
1.4 Denture Fabrication Techniques.....	8
1.4.1 Conventional Techniques	8

1.4.2 Comparison of Compression Molding with Injection Molding Technique	10
1.4.3 Digital Dentures (CAD/CAM)	11
1.5 Comparison between Conventional, Milled and 3 D Printed Denture Bases.....	16
1.5.1 Retention.....	16
1.5.2 Accuracy and Reproducibility	17
1.5.3 Residual Monomer Content.....	18
1.5.4 Physical and Mechanical Properties	19
1.5.5 Color Stability.....	20
1.5.6 Number of Appointments	21
1.5.7 Cost.....	22
1.5.8 Candida Colonization	23
1.6 Effect of Water Storage on Denture Bases	26
1.7 Fractures of Denture Bases.....	26
1.8 Fracture Toughness of Denture Bases	28
1.9 Notchless triangular prism (NTP) specimen K_{IC} test	29
Chapter 2: Research Question and Specific Aim	31
2.1 Research questions	31
2.2 Aim	31
2.3 Null Hypotheses (H_0).....	31
Chapter 3: Materials and Methods.....	32
3.1 Test Materials:	32
3.1.1 Lucitone 199 (C) Denture Base	32

3.1.2 Lucitone 199 CAD (M) Denture Base.....	33
3.1.3 Lucitone Digital Print (P) Denture Base.....	33
3.2 Processing of denture bases for sample preparation.....	34
3.2.1 Lucitone 199 Denture base resin group (C).....	34
3.2.2 Lucitone 199 CAD Denture Base Disc Group (M)	36
3.2.3 Lucitone 3D Print Denture Group (P):	37
3.3 Sample Size Calculation	39
3.4 K_{IC} Test.....	40
3.5 Specimen Preparation	40
3.6 Water storage and conditioning.....	42
3.7 Notchless Triangular Prism (NTP) Specimen Fracture Toughness Test.....	43
3.8 Statistical Analysis	45
3.9 Scanning Electron Microscopy.....	46
Chapter 4: Results	47
4.1 Fracture Toughness (K_{IC})	47
4.2 Crack Propagation and Arrest.....	50
4.3 Work of Fracture	58
4.4 SEM Analysis.....	59
4.5 Weibull Statistics	63
Chapter 5: Discussion.....	65

5.2 Could the notchless triangular prism (NTP specimen K_{IC} test be a better alternative to the SENB test currently recommended by ISO for the determination of fracture toughness of denture base materials?.....	69
5.3 Clinical Significance.....	70
5.4 Limitations and Future Considerations.....	70
Chapter 6: Conclusion.....	71
Bibliography	72

List of Tables

Table 1: Classification of denture bases (ISO 20795-1).....	3
Table 2: Classification according to method of processing.....	4
Table 3: Summary Table Comparing Conventional Denture with CAD-Milled and CAD-3D Printed Dentures.....	24
Table 4: Materials	32
Table 5: Lucitone 199 (C) Denture Base Composition	32
Table 6: Lucitone 199 CAD (M) Denture Base Composition	33
Table 7: Lucitone Digital Print (P) Denture Base	34
Table 8: Results (Mean \pm SD) [#]	47
Table 9: Work of Fracture (WOF) (in KJ/m ²).....	58
Table 10: Weibull Modulus (m) and Characteristics Weibull Fracture Toughness (K _{IC})	63

List of Figures

Figure 1: Chemical formula of methyl methacrylate and poly(methyl methacrylate)	6
Figure 2: Success Injection System (Dentsply International, Inc.)	9
Figure 3: CAD/Milled Denture Base Processing (51).....	12
Figure 4: 3D Printed dentures using SLA technology.....	15
Figure 5: NTP testing assembly (135).....	30
Figure 6(a), (b): Finished acrylic bars fabricated by the (C) injection molding method.....	36
Figure 7: Lucitone 199 CAD Disc.....	36
Figure 8: CAD file designed using AutoDesk Fusion 360 Software	37
Figure 9: STL file for printed samples	38
Figure 10 (a), (b): Printed triangular prisms.....	38
Figure 11: Custom Cutting Jig.....	41
Figure 12: Isomet saw.....	41
Figure 13: Custom Grinding Jig	42
Figure 14: Samples being aged in an Incubator.....	42
Figure 15: NTP specimen custom holder	44
Figure 16 (a), (b): Custom Mounting Jig.....	44
Figure 17: Test Assembly.....	45
Figure 18: Box Plot.....	48
Figure 19: Scheffé post hoc K_{IC} 7 d	49
Figure 20: Scheffé post hoc K_{IC} 90 d	49
Figure 21: Load/Displacement graph for C group at 7 d and 90 d.....	52
Figure 22 (a), (b): Crack Propagation and arrest in C specimens at 7 d and 90 d.....	53

Figure 23: Load/Displacement graph for M group at 7 d and 90 d	54
Figure 24 (a), (b): Crack Propagation and arrest in M specimens at 7 d and 90	55
Figure 25: Load/Displacement graph for P group at 7 d and 90 d	56
Figure 26 (a), (b): Crack Propagation and arrest in P specimens at 7 d and 90 d	57
Figure 27 (a), (b): SEM images - C 7 d at 25x (a) and 150x (b) magnification	60
Figure 28 (a), (b): SEM images - C 90 d at 25x (a) and 150x (b) magnification	60
Figure 29 (a), (b): SEM images - M 7 d at 25x (a) and 150x (b) magnification	61
Figure 30 (a), (b): SEM images - M 90 d at 25x (a) and 150x (b) magnification	61
Figure 31(a), (b): SEM images - P 7 d at 25x (a) and 150x (b) magnification.....	62
Figure 32 (a), (b): SEM images - P 90 d at 25x (a) and 150x (b) magnification.....	62
Figure 33: Weibull Plots for the tested materials	64

List of Equations

Equation 1: Lehr's Rule of Thumb.....	39
Equation 2: Two-parameter Weibull statistics	39
Equation 3: Calculation of K_{IC}	43
Equation 4: Weibull formula.....	45
Equation 5: Calculation of WOF	58
Equation 6: Requirement to ensure plane strain conditions	67

List of Abbreviations

2D	Two-dimensional
3D	Three-dimensional
C	Conventional denture base
CAD/CAM	Computer-aided design/Computer-aided manufacturing
CNC	Computer numerical control
CNSR	Chevron-notched short rod
FDA	Food and Drug Administration
ISO	International Organization for Standardization
IUPAC	International Union of Pure and Applied Chemistry
J	Joule
kN	Kilo Newton
M	Milled denture base
MPa	Mega Pascal
N	Newton
NTP	Notchless triangular prism
PMMA	Poly(methyl methacrylate)
P	Printed denture base
SA	Surface Area
SD	Standard deviation
SEM	Scanning electron microscopy
SENB	Single-edge notched beam
SiC	Silicon carbide
SPSS	Statistical Package for the Social Sciences

STL	Standard Tessellation Language
Wc	Weibull characteristic value
WOF	Work of fracture
wt	Weight

List of Symbols

a	Crack length
α	Significance value
B	Specimen thickness
β	Power
D	Specimen diameter
K	Stress intensity factor
K_{IC}	Fracture toughness (critical stress intensity factor in Mode I loading)
m	Weibull modulus
n	Number of samples
\ln	Natural logarithm
P_{max}	Maximum load
P_f	Probability of failure
T_g	Glass transition temperature
μ	Mean
μm	Micrometer
W	Specimen length
Y^*_{min}	Dimensionless stress intensity coefficient factor minimum
Δ	Standardized difference
σ_y	Yield strength

Acknowledgements

“The mediocre teacher tells. The good teacher explains. The superior teacher demonstrates. The great teacher inspires.” – William Ward

My sincere gratitude goes to Dr. N. Dorin Ruse, who has accepted me under his wings. He is an inspiring teacher who has guided me throughout this journey and taught many valuable lessons, both professional and personal. He has always taken time from his busy schedule to address my concerns. I am forever indebted for his unconditional support, encouragement, and constructive feedback that has enabled me to accomplish my goals. I cannot thank him enough for everything.

I would also like to thank my committee members, Dr. Nesrine Mostafa and Dr. Tom Troczynski, who have offered their constant support and critical feedback during our committee meetings. Your insightful comments have allowed me to complete this project with much ease.

I would also like to thank my fellow residents and my Prosthodontics faculty members for their constant support and encouragement throughout this journey. It has been a pleasure working with you all.

Lastly, thanks to my family members who have been my pillar of strength and support throughout these years.

Dedication

To my lovely wife Kiran and my family who have always believed and supported me throughout this journey.

To all the amazing teachers who have inspired, supported, guided, and helped shape me into the person I am today.

Chapter 1: Introduction

Complete dentures are the minimally invasive and cost-effective option for full mouth rehabilitation of edentulous patients.(1) It has been projected that by 2050, 8.6 million individuals (~2.5 % of the population) in US will suffer from edentulism (2) and a significantly greater percentage in developing countries.(3) Historically, various materials have been used in the fabrication of dentures, including bone, ivory, wood, vulcanite, metals and polymers.(4) Developed in 1937, poly(methyl methacrylate) (PMMA) has ever since been used as denture base material. The polymer has been modified numerous times to improve its mechanical and chemical properties as well its working properties, to adapt to various denture fabrication techniques.(5)

Various fabrication methods are available for complete dentures. The main goal of each of these fabrication methods is to produce denture prostheses with excellent mucosal adaptation, providing good stability, support and retention.(6) The three popular conventional denture fabrication techniques are compression molding, fluid resin pour and injection molding. The compression molding technique, so called “Pack and press”, has been the most widely used technique. The pour technique, as it is less time consuming, has increased in usage. However, some undesirable features of this technique are the movement of teeth during processing, poor tooth bond with the acrylic denture base and air entrapment.(4)(6)

There has been continuous improvement in the fabrication techniques to eliminate the drawbacks associated with conventional techniques and to enhance the properties of the denture base materials. The introduction of computer-aided design/computer-aided manufacturing (CAD/CAM) technology in dentistry, in the early 1980s, has revolutionized the dental field.(7) CAD/CAM has been able to overcome and eliminate some of the problems associated with

conventional denture fabrication.(8) Various CAD/CAM prosthetic systems have been introduced into the market, such as AvaDent, Dentca, Weiland, Ceramill and Baltic Denture system.(9)

1.1 History of Denture Bases

Denture base materials have undergone a paradigm shift over the last 150 years.(10) Before the start of the 19th century, dentures were primarily made from wood, ivory, bone, porcelain and even the currently used metal alloys.(11) However, high cost, patient dissatisfaction, requirement for precise technique and skilled dentists shifted the focus from these materials towards plastic materials.(12) Plastic materials were not only economical but could also render a greater degree of precisions.(12) Vulcanized rubber (Vulcanite) was introduced in the middle of the 19th century as a denture base material. This material eventually shifted the focus towards polymers as denture base materials.(13) In the 1930's, PMMA was introduced as dental base material due to significantly improved physical, chemical, biological, esthetic and handling properties.(5) PMMA was introduced as injection molded material by Imperial Chemical Industries Ltd. in 1935. Kulzer and Co. patented the dough moulding process and marketed a denture base material called Paladon, supplied as powdered PMMA and liquid monomer (methyl methacrylate). When mixed, the powder - liquid forms a dough which is packed into the dental mould and polymerized using heat activation.(11)(14)

Polymers, such as polystyrene, poly(acrylic acid), epoxy resins, polysulphones, polycarbonates, polyamides, urethane dimethacrylate were tested and used as denture base materials, but none could match the excellent properties exhibited by PMMA.(14)(15)(16) Since then, PMMA has dominated as denture base material for denture fabrication.(11) Chemical modifications have been

done over the years to improve the mechanical and physical properties, while still retaining its flexibility to be used as a suitable denture base material.(5)

Digital (CAD/CAM) technology has been developed for the fabrication of complete dentures to overcome and eliminate some of the problems associated with conventional denture fabrication.(17)(18) Various modified PMMA based polymers, such as IvoBase CAD, Lucitone 199 CAD, NextDent 3D+, Lucitone 199 Digital Print, are commercially available to be used with CAD/ CAM systems.(9)

1.2 Classification of Denture Bases

Denture bases can be classified according to the activation of the polymer material and the processing technique.

Table 1 summarizes the classification of denture base materials according to the International Organization for Standardization (ISO) document 20795-1 (19)

Table 1: Classification of denture bases (ISO 20795-1)

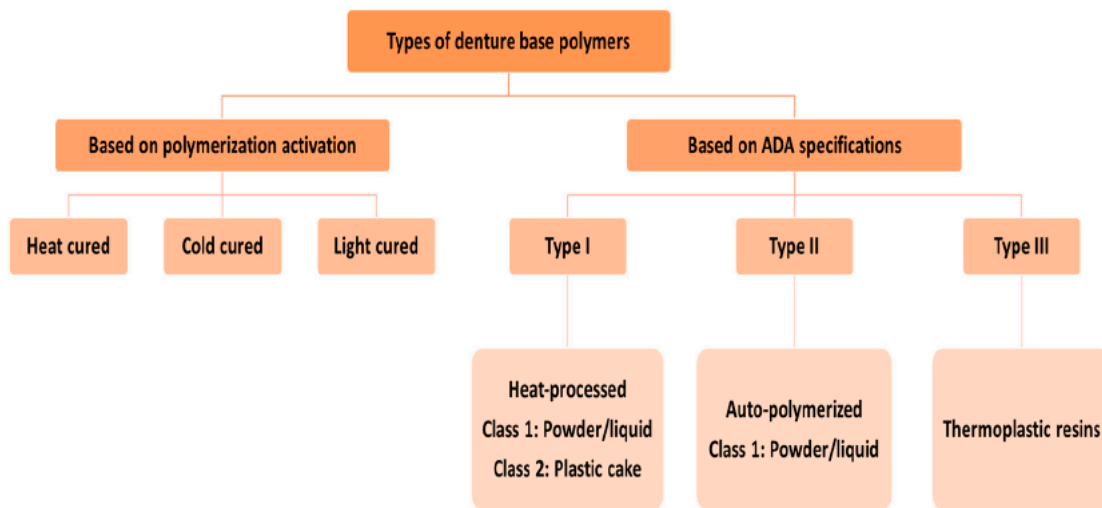
Type 1	Class 1	Heat-polymerizable materials (Powder and liquid)
	Class 2	Heat-polymerizable materials (Plastic Cake)
Type 2	Class 1	Auto polymerizable (Powder and Liquid
	Class 2	Auto polymerizable (Powder and Liquid for pour type resin
Type 3		Thermoplastic blank or powder
Type 4		Light activated materials
Type 5		Microwave cured material

Table 2 summarizes the classification of denture base materials according to the method of processing.

Table 2: Classification according to method of processing

Conventional	Compression Molding
Conventional	Injection Molding
Conventional	Fluid Resin technique
Digital	CAD and milled (Subtractive)
Digital	CAD and Printed (Additive)

The American Dental Association classifies denture base polymers as:(20)



1.3 Poly(Methyl Methacrylate) as Denture Base Material

Poly(methyl methacrylate) (PMMA) is a commonly used polymer in dentistry for the fabrication of denture bases, orthodontic retainers, and denture teeth. As a denture base material, it has been traditionally available as a powder-liquid system.(21) The powder composition is mainly PMMA in which additives, such as pigments, filler particles and synthetic fillers, are added to enhance the esthetic and mechanical properties. The liquid contains methyl methacrylate monomer with the addition of cross-linking and inhibiting agents.(21)(22)

The material gained popularity as a denture base material due to its biocompatibility, repairability, good esthetics, ease of manipulation and cost effectiveness.(5) In spite of these advantages, PMMA has disadvantages, such as low thermal conductivity (0.167-0.25 W/m.K), high-water sorption ($\sim 17 \mu\text{g}/\text{mm}^3$), poor impact (0.02 kJ/m) and flexural strength ($\sim 100 \text{ MPa}$). (23) Several investigations have been conducted on this material to overcome these disadvantages and improves its physical and mechanical properties. The addition of plasticizers, reinforced filler particles, bio-composites and even the modification of the processing conditions (pressure packing, high pressure-high temperature processing) have been attempted.(24)(25)

1.3.1 Poly(methyl methacrylate)

PMMA is a synthetic polymer of methacrylate monomer, with IUPAC name of poly [1-(methoxy carbonyl)-1methyl ethylene] and poly (methyl 2-methyl-propenoate), from hydrocarbon and ester standpoints respectively (Fig. 1).(26) PMMA is a thermoplastic material, exhibiting optical transparency and is widely used due to its high impact strength, easy handling, and processing.(27) Apart from its industrial applications, it has been widely used in biomedical devices.(28)

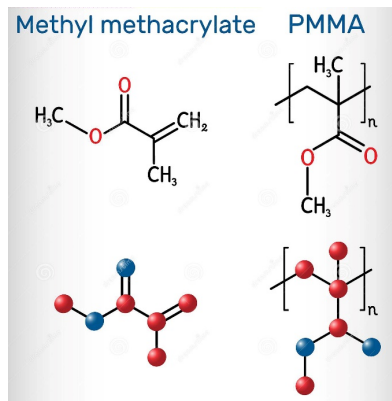


Figure 1: Chemical formula of methyl methacrylate and poly(methyl methacrylate)

[Source: <https://www.dreamstime.com/methyl-methacrylate-mma-poly-methyl-methacrylate-pmma-molecule-methyl-methacrylate-monomer-production-pmma-image189692430>]

1.3.1.1 Physical Properties of PMMA

With regards to its physical properties, PMMA is a colorless, amorphous polymer with a glass transition temperature (T_g) of 100 °C to 130 °C and density of 1.20 g/cm³. The melting temperature of the polymer is 130 °C, with a linear shrinkage of (0.003-0.0065) cm/cm.(29) PMMA has high thermal stability in the range of -70 °C to 100 °C and high resistance to sunshine exposure, rendering it biocompatible.(26) The denture bases should have high thermal conductivity, in order for patients to be able to sense the temperature of the food/drinks. However, PMMA has low thermal conductivity (0.23 W/m·K), which can affect the ability of the patient to sense these changes in temperature.(30) The polymerization shrinkage of the material can result in inaccuracies during denture fabrication.(4) However, PMMA has low polymerization shrinkage compared to other polymers and, therefore, it is still used as a denture bases.(31) PMMA also exhibits low color stability, becoming discolored over long periods of time in the oral environment. Various pigments can be added to PMMA to mask the discoloration and provide adequate esthetics.(32)(33)

1.3.1.2 Mechanical Properties of PMMA

Good mechanical properties are an important requisite for denture base materials to ensure good functional performance, since they are subjected to complex masticatory forces in the mouth.(32) With respect to mechanical properties, PMMA has Young's modulus of ~ 3 GPa.(29)(34) Studies have reported good flexural strength (~ 66 - 78 MPa) of PMMA denture bases.(26) However, long-term water storage has led to decreased flexural strength. Fracture toughness is an important properties for PMMA to act as denture base material.(26) Studies have reported the fracture toughness of PMMA denture bases to be in the range of (1.84 ± 0.33) MPa \cdot m^{1/2} to (2.11 ± 0.29) MPa \cdot m^{1/2}. (35)(36) The wear resistance of the PMMA is considerably lower than that of metals and ceramics.(37)

1.3.1.3 Biological Properties of PMMA

If properly processed, PMMA has low residual monomer content, therefore good biocompatibility.(38) Any residual monomer remaining can cause allergies, mucosal inflammation, and cytotoxicity.(38) The residual monomer content can be decreased by increasing the degree of polymerization using the recommended processing cycle for PMMA.(38)(39)

1.3.1.4 Chemical properties of PMMA

The chemical resistance is reasonable, PMMA is not affected by most aqueous solutions; however, it is highly soluble in aromatic hydrocarbons, esters, ketones and chlorinated solutions.(26)(29)

1.4 Denture Fabrication Techniques

1.4.1 Conventional Techniques

1.4.1.1 Compression Molding

Conventional compression molding technique is the most widely used technique to fabricate denture bases and is used in conjunction with heat-activated materials. In this technique, an accurate wax trial denture is prepared and packed into a mold. The wax is then eliminated using hot water and detergent and a separating medium, such as sodium or ammonium alginate, is applied. The polymer and monomer are mixed in a ratio of 2:1.(4) Once the material reaches the doughy stage, the flask is closed, using gradual incremental pressure, which helps in distributing the resin throughout the mold space. Once the flask is fully closed, the polyethylene packing sheet is removed, along with excess flash material. The process is repeated till no flash is evident; the flask is closed for the last time under pressure. The flask is then transferred to the flask carrier under pressure. The polymerization reaction is activated by immersing the flask in a hot water bath at a set temperature. The curing can be done either by using a long or a short cycle.(4)

1.4.1.2 Injection Molding

Injection molding technique was introduced in 1942 by Pryor to overcome the problem of polymerization shrinkage by forcing the resin into the processing flask.(40) Ivoclar was the first company to introduce the commercially available injection molding system (SR Ivocap) in the 1970s, (41) with Dentsply following the suit with their Success injection system (Fig. 2).(42) In these systems, capsules containing pre-proportioned polymer and monomer are used. A special flask with a sprue is used to inject the PMMA into the mold cavity using a piston at a set pressure

(8 MPa). The pressure is maintained as the material is slowly injected.(43) Curing is completed in the water bath using the long or short curing cycle.(4)



Figure 2: Success Injection System (Dentsply International, Inc.)

[Source: <https://www.pattersondental.com/en-CA>]

1.4.1.3 Fluid Resin Technique (Pour)

The fluid resin technique (pour) uses a pourable, auto-polymerizing (chemically-activated) resin. This technique utilizes powder and liquid, which when mixed together in proper ratio yield a low viscosity resin. Wax trial dentures are invested in hydrocolloidal material, and the wax is eliminated using a hot water bath. The low viscosity acrylic is poured through sprue channels, under pressure. The flask assembly is placed in a pressure pot at ambient temperature and the resin is allowed to polymerize for 30-45 mins. The resin used in this technique is chemically activated and no use of external energy is needed. Dentures fabricated with this technique are inferior to those processed by compression molding or injection molding techniques.(4)

1.4.2 Comparison of Compression Molding with Injection Molding Technique

Compression molding technique has been associated with numerous disadvantages. Polymerization shrinkage and the dimensional changes associated with it have been much higher than those associated with injection molding.(44) This could lead to problems with adaptation between the denture bases and the oral mucosa, compromising stability and retention.(45) It has also been reported that the compression molding technique can lead to occlusal discrepancies, necessitating a lab remount.(46) Compression molding technique can also lead to increased alteration in the incisal pin opening, leading to time consuming occlusal adjustments and disfigurement of the occlusal anatomy of the artificial teeth.(42) The injection molding technique claims to eliminate these errors and produce dentures that require minimal adjustments.(42) It has been reported that the injection molding technique produces more accurate denture bases with no difference in the laboratory working times.(42)(47) The occlusal adjustments are also minimal for denture produced by injection molding technique.(42) The deformation of the denture bases has also been minimal with injection molding technique compared to that of denture bases processed with the compression molding technique.(43) A study by Clements et al. has also reported increase in mechanical properties of denture teeth processed using the injection molding technique.(41) They also reported that the amount of residual monomer remaining with injection molding technique is less than that in dentures processed with compression molding technique.(41)

1.4.3 Digital Dentures (CAD/CAM)

1.4.3.1 CAD/Milled

Milling is based on subtractive manufacturing, in which a finished product is obtained from a large blank with the use of computer numeric controlled (CNC) machines. The process involves sequencing, milling, tool movements through a series of commands that dictate the CNC machine into a specific direction. Varying sizes of burs are incorporated into the machine and the CAM software controls the bur(s) movement on the desired surface. CNC machines used in dentistry have multi-axis to facilitate the milling of dental prostheses in three dimensions.(48) Depending on the movement of the milling burs (x-, y- and z- axes) and additional rotational axes, these can be divided into 3-, 4- (one additional rotational axis around x- axis) or 5-(two additional rotational axes around x-axis and y- or z- axis) axes milling machines.(49)

3-axis milling machines are the most widely used with the bur moving according to calculated path in 3 axes. The advantage of 3-axis milling machining is that they render a faster milling time and require minimal computation. However, these cannot produce convergence, divergence or highly defined features and surfaces. In addition, the restricted movement of the bur does not allow the production of large prostheses. 4-axis milling machines and its additional rotational axis around the x-axis (A-axis) allows for the milling of larger frameworks and prostheses. The 5-axis milling units allow for two rotational axes of the milling bur or blank. Complex geometries and smooth external surfaces can be produced using these machines.(48)(49) Acrylic denture bases with complex anatomies and smooth surfaces can be produced using 5-axes milling machines.(50)

Final functional impressions are taken, either conventionally or digitally. Once the impressions and prescriptions are transferred into the software, the gingival color base and the teeth set-up is chosen, and CAD is completed according to the protocols. Pre-polymerized disks ("pucks") are then milled using 5-axis CNC machines fitted with suitable burs (Fig. 3).(51) The teeth are attached to the denture bases using bonding agent and the denture is finished and polished according to conventional protocols.(52)



Figure 3: CAD/Milled Denture Base Processing (51)

1.4.3.2 3D Printing

3D printing, is an additive manufacturing process in which an object is created by adding multiple layers of a material to create a three-dimensional object. The process has been widely used in many fields, such as aerospace, engineering, medicine, and architecture. In recent years, in field of dentistry, its use in combination with CAD technology has been revolutionary.(53)(54)

Discretization and sequential stacking are two basic concepts for 3D printing. The CAD complex 3D object has its layers sliced and changed to 2D layers by discretization.(54) The multiple sliced layers have certain layer thickness with information about the contours and the design of the object to be printed.(53) Subsequently, sequential stacking deposits the material in pre-determined form and areas, with layers firmly stuck to the previous, creating the desired 3D model.(54)

There are many rapid prototyping systems available, such as stereolithography (SLA), fused deposition modeling (FDM), selective laser sintering (SLS), inkjet based three-dimensional printing(3DP), laminated object manufacturing (LOM), laser engineered net shaping (LENS).(54) SLA, FDM, SLS and 3DP have been widely adopted for use in dentistry.(55)

Stereolithography (SLA): SLA was the first rapid prototyping system, developed by Charles Hull in 1980's.(56) The process involves building the object layer by layer on the build platform by tracing a beam of ultraviolet (UV) light on top surface of the photosensitive liquid resin. The UV light causes the solidification of the layer of the polymer resin. Subsequent layers adhere to the first solidified layer as the platform is lowered to the next layer thickness. The tracing of the layers continues as the platform is lowered and the solidified layer is coated with new self-adhering resin until the fabrication of the completed object.(54) Power of the light source, the composition and chemistry of the resin and amount of photo initiators, all effect the kinetics and the depth of the polymerization.(53)

This process is widely used in dentistry for the fabrication of surgical guides, denture bases, maxillofacial prosthesis, and study models. The finished objects have high accuracy, good details, good surface finish and good mechanical strength. The disadvantages of this process include expensive equipment, wet handling, and additional post curing.(54)

Selective Laser Sintering (SLS): This process involves the fusion of powdered material, with a CO₂ laser, to produce a 3D object. The measured powdered material is delivered incrementally through the cylinder, with the specific layer thickness, and is spread across the build platform. The laser traces the design on the surface of the powdered material, raising the temperature of the powder particles to their point of melting and ultimately forming a solid object. Modulation of the laser beam is done just as to melt the powder in the geometrically defined areas of the object. The temperature of the powder is maintained below its melting temperature but high enough to cause sintering.(54) Once the first layer is fused, additional layers are deposited by the moving roller on the build platform.(55) The process repeats until the completion of the object.(54) This process requires no post curing cycles. This process is used for the fabrication of metal substructures, ceramics and thermoplastic composite objects.(55)(57)

Fused Deposition Modeling (FDM): In this prototyping technique, a thermoplastic material is extruded layer by layer through a temperature-controlled nozzle. The thermoplastic material is heated to convert it to a semi-liquid state, allowing it to flow. The thermoplastic material solidifies immediately after it is ejected from the nozzle head, bonding to the layer below with precision. The system deposits one layer on top of the other on the build platform, operating in XYZ axes. Any overhangs or supporting structures can be removed by cutting and polishing to achieve the desired object geometry.(54)(55) This process is usually used to manufacture medical grade bone models, surgical stents, etc., using a single manufacturing process. No post cure cycle is needed in this rapid prototyping process.(54)

Three-Dimensional Printing (3DP): The process involves dispensing a measured amount of powder from the supply chamber. The supplied material is distributed and compressed using rollers over the fabrication chamber. A two dimensional pattern of liquid adhesive is jetted onto

the powdered layer, bonding to the powder below to form an object layer. The layers are subsequently added as the build platform moves incrementally and next powdered layer is spread and bonded. The layer-by-layer process continues until the whole object is completed. Any unbounded powder is removed with heat treatment. This technique provides fast fabrication with minimal material cost. However, the finished object lacks resolution, surface finish and adequate strength.(54)

3D Print Denture Fabrication

3-D denture printing technology utilizes digital light processing technology (Stereolithography), in which CAD data builds up a designed structure exposing the photopolymerizable resin liquid layers to ultraviolet light. Computer aided design image is projected through a slit, using a micro-mirror device, followed by projection of ultraviolet light onto the surface of liquid resin. Ultraviolet light polymerizes the layers of photopolymerizable resin leading to bottom up stacking of layers of certain thickness to form a 3-D object followed by a post curing cycle (Fig. 4).(58)



Figure 4: 3D Printed dentures using SLA technology

[Source- <https://www.3dprintingmedia.network/carbon-dentsply-sirona-3d-printed-denture-workflow/>]

1.5 Comparison between Conventional, Milled and 3 D Printed Denture Bases

1.5.1 Retention

Lack of sufficient retention in the prosthesis is one of the most frequent complaints by denture wearers.(59) The retention of complete dentures is dependent of various factors, such as good adaptation to denture bearing area, border seal, surface tension, viscosity and film thickness of saliva.(60) Processing errors during conventional denture fabrication can lead to linear distortion in the denture bases in the range of 0.45 % to 0.9 %.(6) This has negative impact on fit by decreasing proper adaptation to tissues and ultimately reducing the retentive forces.(61) Digital denture fabrication process is an automated process and is able to accommodate error better than the manual processing techniques.(62)

Compared with conventional denture bases, significantly higher reproducibility and tissue adaptation has been reported for CAD/CAM milled dentures. CAD/CAM had the smallest dimensional distortion, almost zero, and was the most reproducible processing technique.(6) Conventional techniques lead to volumetric changes during processing due to shrinkage.(6) The milled dentures, on the other hand, are processed from fully polymerized, higher density pucks, and show no distortion and better adaptation.(63)(64) There are only few studies comparing the adaptation of 3-D printed dentures with that of milled dentures. Chen et al. have reported that 3-D printed dentures have comparable tissue adaptation to that of milled dentures.(65)

It has also been reported that digital dentures produce adequate mucosal compression, required for retention, without inducing inflammation of the tissues and are much more acceptable clinically than conventional dentures.(66) It has been found that 3-D printed dentures had better tissue adaptation than milled.(65) 3-D printed denture fabrication was able to reproduce residual ridge

irregularities better than milled denture fabrication, thereby resulting in better tissue adaptation and retention. The surface adaptation of 3-D printed denture has been within 100 μm accuracy.(58)

1.5.2 Accuracy and Reproducibility

During the fabrication of dentures using the heat curing method, there is tendency of the palatal aspect to move towards the cast and for the borders to lift.(67) It has been reported that as the denture lifts from the model, there is increased dimensional changes between the denture and working cast.(68) The fabrication process with conventional fabrication techniques involves time consuming procedures, such as waxing, investing, and wax elimination, each incorporating some errors, leading to decreased accuracy.(69) In addition, residual stress incorporated during the packing is released during the removal, causing the finished denture base to shrink, resulting in the displacement of the denture teeth, leading to inaccuracies in the occlusion and poor fit. In case of maxillary dentures, the maximum amount of shrinkage occurs in the center of the palate.(70) CAD/CAM processing eliminates uncontrollable manual processing errors.(62) Therefore, the CAD/CAM fabrication process is more accurate as compared to conventional procedures.(6) However, a study comparing the deformation of denture bases and the influence of arch shape and palatal vault on shrinkage have found that CAD/CAM milled dentures are equally well fitting to dentures processed by injection molding and better than those processed by compression molding techniques.(71)

In 3-D printed dentures, additive technology is employed and the denture base is layered in thin resin layers with no lifting from the model as the process is digitally controlled.(70) The accuracy of the light cured resin layered with additive technology is superior to that obtained by conventional heat-curing methods.(70)(31) The mean value of discrepancy measured in the mid-

palatal suture area between the maxillary denture and the working cast was reported to be lowest in the 3-D printed group, followed by milled and injection molding groups.(72)

3-D printed digital denture offer added advantages, such as the ability to bypass deep undercuts, to obtain finer reproduction details, be faster, have lower anisotropy as well as lower material costs.(73) The accuracy of printed dentures is influenced by factors such as intensity of light, orientation and print angle, printing software, number of layers, supporting structure, postprocessing techniques, shrinkage between layers and offset between teeth and denture recesses.(72) Different 3-D print resins have their own activation ranges and require different light wavelength and exposure time for polymerization. Compatibility of resin material with all available 3-D printers is also an issue.(72)

1.5.3 Residual Monomer Content

The presence of remaining unreacted residual monomer is highly undesirable as it can compromise the mechanical and physical properties of the denture bases as well their biocompatibility.(74) Residual monomers are likely to leach into the surrounding tissues, leading to cytotoxicity and possible responsibility for allergic reactions. Burning mouth sensation, denture stomatitis, tissue edema, ulceration of the oral mucosa are some of the symptoms associated with residual monomer leaching into oral cavity.(74)(75)

The amount of leached residual monomer is directly proportional to the concentration of remaining monomer within the processed resin. Hence, increasing the degree of conversion of residual monomer is desired, which depends upon the curing methods, temperature, pressure application and processing time.(74)(76)(77)

Conventionally fabricated denture bases have been shown to release residual monomer into the surrounding environment, with significantly higher amounts released from chemically-cured than from heat-cured dentures, associated with the degree of polymerization achieved.(78) Digitally milled dentures are fabricated by milling from polymethylmethacrylate pucks that have been pre-polymerized under high pressure and temperature.(79) These conditions lead to higher degree of monomer conversion as well as formation of longer polymer chains, leading to lower residual monomer content.(80) It has also been hypothesized that since CAD/CAM processes eliminate the human impact on processing, there have been greater standardization of the processes involved, leading to higher degree of polymerization, lower porosity and increased mechanical properties.(74) A study comparing the CAD/CAM denture bases with conventional denture also reports that higher material thickness of the pre-polymerized PMMA puck might also prevent the leaching of the residual monomer from the center, which often is milled as the denture surface. The results of the same study reported that lower monomer release from CAD/CAM was statistically significant when compared to auto-polymerizing conventional dentures.(74) No available literature is available comparing the release of residual monomer from printed denture bases over long term.

1.5.4 Physical and Mechanical Properties

Dentures can break upon impact, so it is necessary for them to have a higher impact strength.(81) Better mechanical properties may also allow for dentures to be fabricated without need for any additional strengthening through metal or fiber reinforcement. High modulus of elasticity can prevent crack propagation.(82) Dentures can then be fabricated with minimal thickness without incidents of fracture and thereby increasing patient comfort. Patients will experience more natural

speech and feel as the denture requires less volume within the oral cavity.(83) The resins materials used for conventional and digital denture bases are chemically similar, however they differ in the process of production. The mechanical properties of digital dentures are distinctly different from those of conventional dentures.(83) Digital dentures possess increased impact strength, ultimate strength and higher modulus of elasticity.(79)(81)(84) These can be explained as CAD/CAM PMMA pucks are manufactured under high pressure and temperature resulting in minimal shrinkage, porosity and free residual monomer.(79)(81) However, results of another study reported higher flexural strength for CAD/CAM milled dentures but lower for 3D printed dentures.(81) Surface hardness of the CAD/CAM dentures has also been reported to be higher than that of conventional dentures, preventing mechanical damage, retention of plaque and stains and increasing life of the dentures.(81)(85)

1.5.5 Color Stability

Color stability is an important clinical feature of denture bases. To create an esthetic appearance, color and appearance matching to the underlying tissues is required of denture base materials.(86) Color change is a major cause of patient dissatisfaction with prosthesis and reason for replacement.(87) Aged and worn dentures show changes in color, leading to unaesthetic appearance.(88) Water sorption, physical and chemical changes, accumulation of stains due to exposure to foods and beverages (coffee, spices, wine etc.) and increased surface roughness can affect the color of the denture bases.(89) Red wine has been shown to have greater effect on the color due to its acidic pH as well as the alcohol content. Alcohol can lead to softening of the material, changing the surface smoothness and causing expansion of polymer chains, leading to higher absorption of pigments.(90)(91) Resin composition and method of polymerization can also influence color stability.(92) Conventional denture bases processing is dependent upon the

technician for proper material mixing ratio, processing time, which can affect color stability.(93) On the contrary, CAD/CAM processing relies on industrially pre-polymerized pucks, which have better mechanical properties, less porosity, less residual monomer, less water sorption and show less wear. All these factors lead to a better color stability in CAD/CAM dentures.(94) A study has also reported that the greatest susceptibility to color change is the interface between the prosthetic teeth and the denture base due to effects of polymerization shrinkage.(95) Stains and microorganisms can penetrate this interface leading to discoloration.(95)

1.5.6 Number of Appointments

Difference in the number of appointments has been reported for dentures fabricated via digital and conventional processing. There are various commercially available companies, such as Weiland (Ivolcar), AvaDent, Dentca and Ceramill. Each of these companies have their own protocol for digital denture fabrication, appointments ranging from 3 appointments (Weiland (Ivolcar), AvaDent, Dentca) to 4 appointments (Ceramill), which is still less than the 5 appointments required for conventional dentures. It has been reported that digital dentures require a mean 2.39 appointments to delivery compared to 5 appointments for conventional denture, with no influence of operator experience level.(96) Another study reported that digital dentures can be delivered in 2 appointments even by students in predoctoral setting under faculty supervision.(97) A significant reduction in clinical time by 3.5 hours compared to conventional dental fabrication has also been reported.(97) This reduction in clinical time can be utilized to ensure good outcome through good laboratory communication and provide more effective treatment.(96)(98)

Misfit range for CAD/CAM denture bases was lower than for those of conventional technique. Therefore, it can be postulated that there will be less need for postinsertion appointments for

CAD/CAM dentures will also be less. Bidra et al reported patient centered and clinical results of 2 appointment CAD/CAM denture bases and found that an average of 3.3 denture adjustments were needed for CAD/CAM denture bases.(98) Another study, however, reported no significant difference in the number of appointment for conventional or digital denture bases.(99)

1.5.7 Cost

There have been studies supporting that the number of appointments required for digital dentures are less than that for conventional dentures.(96)(97)(98) However, none of these studies have quantitatively determined the cost of each processing technique. A study by Srinivasan et al. compared the cost of digital denture fabrication with conventional denture and found that the overall cost of digital denture is approximately 50 % less than that of conventional denture.(100) They have also reported that in spite of higher clinical material cost initially, the laboratory costs are significantly reduced.(100) During their cost minimization estimation, an estimated ten-year profit of about \$150,000 was determined within a university setting with digital dentures over conventional dentures.(100)

However, the initial cost of milling units is higher than that of the 3-D printers and more suitable for commercial manufacturing rather than for small dental laboratories. The amount of energy consumption is also significantly higher. Subtractive milling is less environmentally friendly as it leads to material waste, thereby contributing to environmental pollution. Despite the high cost, small desktop and intraoral scanners can be afforded by individual dentists and small laboratories. These scanners can be connected to digitally print in house 3-D dentures, thereby avoiding delays in delivery and shipping costs.(101)

1.5.8 Candida Colonization

Colonization by *Candida* in denture wearers has been established as one of the predisposing factors for denture stomatitis.(102) The adhesion of *Candida* to the denture occurs through the adhesion of biofilm to the denture and also on surface irregularities present on the denture.(103) Conventional processing techniques result in surface porosity due to air entrapment, uncontrolled temperature, evaporation of monomer, inadequate pressure and residual monomer content.(104) This can result in porosity and roughness and can lead to adherence of *Candida* species.(105) Since CAD/CAM dentures are processed from pre-polymerized pucks, there is less porosity and a better surface finish, leading to decreased adherence of *Candida*.(106) Bidra et al. also reported decrease adhesion of *Candida* with CAD/CAM denture surface due to decreased porosity.(98) Conventional denture bases also need to be stored in water as hydration negates the effect of polymerization shrinkage and establishes equilibrium with residual monomer content.(4) CAD/CAM denture experience less distortion, hence water storage can be avoided. A recent systematic review has found that *Candida* growth is slower on the surface of dry dentures.(107)

Table 3: Summary Table Comparing Conventional Denture with CAD-Milled and CAD-3D Printed Dentures

Outcome	Conventional	CAD- Milled	CAD-3D Printed
Retention	Low	High	High
Accuracy & Reproducibility	Low	High	High
Residual monomer release	High	Low	Low
Tooth movement and Occlusal discrepancies	High	Low	Low
Color Stability	Low	High	High
Patient satisfaction	Low	High	High
Esthetics	High	Low	Low, but higher than milled
Number of appointments	More (5)	Less (3)	Less (3)
Post insertion appointment	More	Less	Less
Clinical Time	More	Less	Less
Cost	High but with low initial material cost	Low with high initial material cost	Low with high initial material cost

Outcome	Conventional	CAD- Milled	CAD-3D Printed
Mechanical Properties	Inferior to CAD/CAM milled but superior to printed	Superior to Conventional	Inferior to both milled and conventional
Chances of Fractures	High	Low	Low
Electronic storage and archive	Absent	Present Data be Electronically stored and used at later date	Present Data be Electronically stored and used at later date
Denture adhesive	Increases retention	Decreases retention	Decreases retention
Biocompatibility	Low	High	High
Special equipment	No special equipment required	Required	Required
Processing	Manual	Automation	Automation
Tooth Bonding to denture base	Chemical during the processing. No special bonding agent needed.	Special bonding agent needed to bond teeth with denture base recess	Special bonding agent needed to bond teeth with denture base recess
Duplication	Need more clinical and laboratory steps	Can be done in 1 appointment	Can be done in 1 appointment
Deep Undercuts reproduction	Easy	Difficult	Very easy

Outcome	Conventional	CAD- Milled	CAD-3D Printed
Material Waste	High	High	Low
Operator skills/experience	High skills and experience needed to build good dentures	Not required	Not required

1.6 Effect of Water Storage on Denture Bases

Water sorption is one of the disadvantages associated with PMMA material being used as denture base materials. Water molecules can easily penetrate the PMMA polymer chains and act as plasticizer, causing expansion and dimensional instability.(108) The dimensional stability of the PMMA material is related to its solubility as well.(18) ISO 20795-1 recommends that the water sorption and solubility of the denture base material to be less than $32 \mu\text{g}/\text{mm}^3$ and $1.6 / \mu\text{g}/\text{mm}^3$, respectively.(19) Most commercially available denture materials fulfil these minimum requirements.(19) Water sorption also effects the color stability of the denture bases. Water sorption and solubility are directly affected by the residual monomer content.(32) The higher the residual monomer content, the higher is the water sorption and solubility of the denture base materials. Since the residual content of the CAD/CAM and 3-D printed denture material is less than that of conventionally fabricated denture bases, the dimensional changes in the former are lesser than those of the latter.(74)

1.7 Fractures of Denture Bases

Denture bases do not fracture just from the obvious direct trauma/fall, but also due to the flexural fatigue that sets in over repeated use.(109)(110) A denture base is flexed millions of times during

its use. Maxillary denture flex as much as 1.5 mm, while mandibular denture flex in a range of 1.5 mm to 3.6 mm during the masticatory cycle, with the maximum in the midline area.(109) The average fracture rate in removable dentures is as high as 68 %.(111)(112) Clinical surveys have shown that the most common fractures in denture bases are midline fractures.(111) Occlusal forces lead to the development of microscopic breaks or cracks in the denture base. Under repeated stress, this crack continues to grow, eventually leading to the catastrophic fracture of the denture base.(113)

Sharp frenal notch, diastema and presence of tori can increase the incidence of the fractures by introducing stress concentrators.(111)(114) Finite element stress analysis investigations have found that longer and sharper frenal notches can result in higher concentration of stress, thereby in higher chances of fracture initiating from these areas.(114)(115)(116). Notch geometry has been shown to play an important role in the nature of stress occurring in denture bases. A shallow, smooth notch has higher tensile forces acting than a deep and sharp frenal notch.(111)

PMMA has been widely and efficiently used as the denture base materials since decades. However, the material has poor impact strength and low fatigue resistance, thereby fracturing often.(117)

1.8 Fracture Toughness of Denture Bases

Denture bases are subjected to various stresses while functioning in the mouth.(118) The presence of surface flaws on the denture bases can act as stress concentrators leading to crack propagation and ultimate failure of the denture bases.(119) A denture base material should be able to resist crack propagation and withstand surface flaws to produce a strong and fracture resistance denture, enhancing longevity and clinical performance.(120)

Fracture mechanics methodology can be used to measure the resistance of denture base to crack propagation.(121) Fracture toughness (K_{IC}) is an intrinsic material property, characterizing the ability of a material to resist unstable crack propagation, caused by internal flaws, under applied force (tension).(122) Hence, requirement of adequate K_{IC} is an important requirement for denture bases.(122)

Chevron notched short road (CNSR) specimen (123), tapered cleavage specimen (124), single edged notched beam (SENB) specimen (125) and notchless triangular prism (NTP) specimen (126) K_{IC} tests have been used to determine K_{IC} of denture base materials.

1.8.1 Appropriateness of K_{IC} testing in denture bases:

Clinical failure of the denture bases is a slow process; therefore, K_{IC} testing is more appropriate than impact strength testing. Impact strength is dependent of geometry and loading conditions, while K_{IC} is independent of these factors and dependent only on the tested material.(127)(128) Thus, to assess the ability of a material to resist fracture, K_{IC} is a reliable quantitative method.(129)

1.8.2 Challenges to conducting K_{IC} in denture bases:

Studies have been performed on polymers to predict the degree of stress intensity at the flaw tip, which lead to crack initiation.(130) Due to the heterogeneity of the available denture base materials, K_{IC} values differ for individual denture bases materials.(131) Molecular weight and degree of cross-linking in denture base materials can also affect K_{IC} . Depending on the method of fabrication, each type exhibits different degree of brittleness, due to differences in crosslinking, molecular weight, viscoelasticity and chemical composition of the matrix.(118)(132) Application of fracture mechanics is quite complex for denture bases, as crazing and development of plastic zone can occur around the crack tip.(133)

1.9 Notchless triangular prism (NTP) specimen K_{IC} test

CNSR test, introduced by Barker, has been a commonly used method to determine K_{IC} of brittle materials.(123) The method was subsequently modified to accommodate small samples of dental relevance.(134) However, there are several disadvantages of this method as it is much more technique sensitive, difficult to control with small brittle material sample and error prone in characterization of adhesive interfaces.(126) In 1996, Ruse et al. developed and validated a novel method to determine K_{IC} of various dental materials, as well as of bonded interfaces, while retaining the overall CNSR geometry (Fig. 5).(126)

The NTP specimen K_{IC} test is detailed in the materials and methods section (Pg. 44).

There are several advantages of this methods, as the specimen preparation is simple and reproducible, allows testing of materials with $K_{IC} < 1 \text{ MPa}\cdot\text{m}^{1/2}$, can be applied to various materials

and interfaces, provides controlled and stable testing conditions, and results in values comparative to those obtained by CNSR testing.(126)

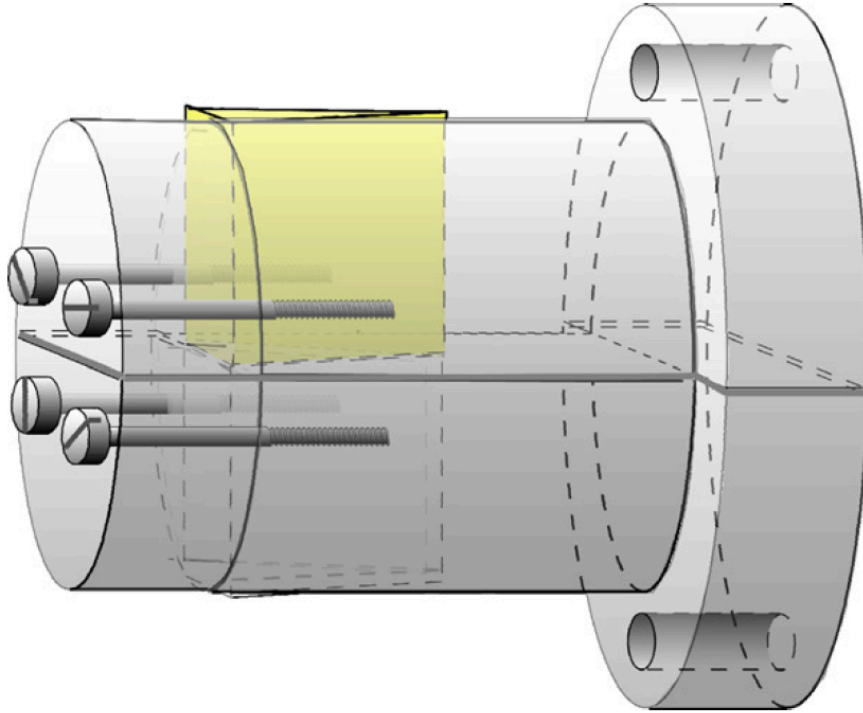


Figure 5: NTP testing assembly (135)

Chapter 2: Research Question and Specific Aim

2.1 Research questions

- Do newly developed CAD/CAM [Milled (M)] and 3D-printed (P) denture base materials have improved fracture toughness (K_{IC}) compared to conventionally processed (C), counterparts?
- Does long-term water storage effect K_{IC} of the denture bases?

2.2 Aim

The aim of this project was to use the NTP specimen K_{IC} test (126) to determine K_{IC} of a conventionally fabricated denture base material and compare it with that of CAD/CAM and 3D-printed materials. K_{IC} was determined after storing the samples in 37 °C water for 7 d and 90 d. The guidelines of ISO 20795-1 (19) were followed for the ageing and conditioning of the samples prior to testing.

2.3 Null Hypotheses (H_0)

- There is no difference between K_{IC} of the three different denture base materials investigated.
- There is no effect of long-term storage in 37 °C water on the K_{IC} of the three different denture base materials investigated.

Chapter 3: Materials and Methods

3.1 Test Materials:

For this study, the test materials were kindly donated by Dentsply International Inc. (Dentsply International Inc., York, PA), Table 4 lists the materials used in this study.

Table 4: Materials

Materials	Lot	Manufacturer
Lucitone 199 Denture Base Resin (C)	015822	Dentsply International Inc., York, PA
Lucitone 199 CAD (M)	180222	
Lucitone Digital Print (P)	NA	

3.1.1 Lucitone 199 (C) Denture Base

Lucitone 199 Denture base resin has been a Dentsply Inc. proprietary resin since the 1980s. Available in different shades and translucency, it has been extensively used by laboratories and clinicians for denture base fabrication. The materials come in an inactivated powder and liquid form, which, when mixed together in a ratio of 2:1, results in a homogenous polymer resin to be used as denture base material. Table 5 lists the components and their composition.

Table 5: Lucitone 199 (C) Denture Base Composition

Component	Composition	Weight %
Powder	Poly(methyl methacrylate)	(90-100) %
Liquid	Methyl methacrylate	(80-100) %
	Ethylene dimethacrylate	(1-2) %

3.1.2 Lucitone 199 CAD (M) Denture Base

Lucitone 199 discs are used in CAD/CAM digital denture base fabrication. Available as pre-polymerized 98.5 mm diameter discs of various heights (20 mm, 25 mm, 30 mm, or 35 mm), enabling the laboratories to mill them directly into denture bases. They maintain dimensional stability under high-speed milling and offer a clean, safer way to fabricate denture bases to which acrylic teeth can be bonded or milled together. Table 6 shows the chemical composition of these discs.

Table 6: Lucitone 199 CAD (M) Denture Base Composition

Components	Weight (Wt) %
Polymer blend * [mainly poly(methylmethacrylate)]	(>99) %

* The exact concentration of components is withheld by Dentsply as trade secret.

3.1.3 Lucitone Digital Print (P) Denture Base

Lucitone Digital Print is a novel light-cure resin material developed by Dentsply. It has received FDA approval in 2019 for the fabrication of digital denture bases. Fabrication of prosthesis using this material requires a CAD system and an additive 3D printer. Carbon 3D Digital printers have been optimized for this resin material and require wash and light cure post processing. Similar to Lucitone 199 discs, it requires chemical bonding to adhere denture teeth to the base. Table 7 lists the chemical composition of the resin.

Table 7: Lucitone Digital Print (P) Denture Base

Components	Weight (Wt) %
Urethane Methacrylate	(40-50) %
Methacrylate Monomer	(40-50) %
Acrylate monomer	(1-5) %
Photoinitiator	(1.5) %

3.2 Processing of denture bases for sample preparation

3.2.1 Lucitone 199 Denture base resin group (C): Horizontal bars measuring [(65x20x10) mm] were prepared in the lab by stacking layers of baseplate wax (Dentsply TruWax, York, PA). The horizontal wax bars were finished, polished and made ready for investing in the plaster. Commercially available flasks were used with the SUCCESS injection system after application of petroleum jelly for easy release. Type 3 dental stone (Microstone, Whipmix, Louisville, KY) was mixed in manufacturer specified water: powder (40 ml: 140 g) ratio, poured into the dental flask and the wax bars were embedded in it. Any undercuts present were eliminated, and Success Sprue Wax was used to build the injection sprue on one side of the investment flask. Separating medium (Petroleum jelly) was applied after the stone had set. The upper half of the flask was attached to the lower half. Type 3 dental stone (Microstone, Whipmix, Louisville, KY) was mixed and poured to cover the remaining top half of the flask and allowed to set completely.

The injection flask was placed in boiling water for (6 to 10) min to soften and eliminate the wax. The flask was opened after complete wax boil-out, removing and discarding the remaining wax.

The residual cavity and the flasks were flushed and cleaned thoroughly to remove any remaining wax residues. The cavity and the margins of the flask were verified for intimate contact. Two coats of alginate separating media was applied to the dental stone before the acrylic was packed into the flask.

The injection flask was attached to the Success injection system using metal injection insert, as per instructions. As per manufacturer instructions, Lucitone 199 powder (17 g) was mixed with the liquid monomer (8 ml) and stirred for 15 sec. in order for the powder particles to be completely wetted. Once the material reached “soft pack” stage, it was loaded into the injection cartridge. The flask was placed into the injection unit and positioned using the “O” ring and tightened. Once the flask was secured and aligned vertically, the activation switch of the injection unit was turned on and acrylic material was injected into the flask. A pressing device with piston was attached to the injection socket and kept in assembly for a couple of minutes.

The flask was allowed to cool on bench top for 30 min to avoid porosities. The flask was put in a water bath for heat curing, using the long cycle at temperature of 73 °C for 9 h, followed by bench-top cooling for 30 min. The flask was unscrewed, the top half of the investment flask was separated from the bottom half and the processed acrylic bar was removed from the flask. The excess flash from the bar was removed and final finishing and polished was done using acrylic burs and wheels. Fig. 6(a) and (b) show the finished acrylic bars fabricated by the conventional injection molding method. The NTP specimens were prepared from these bars by cutting, finishing and polishing to required dimensions.

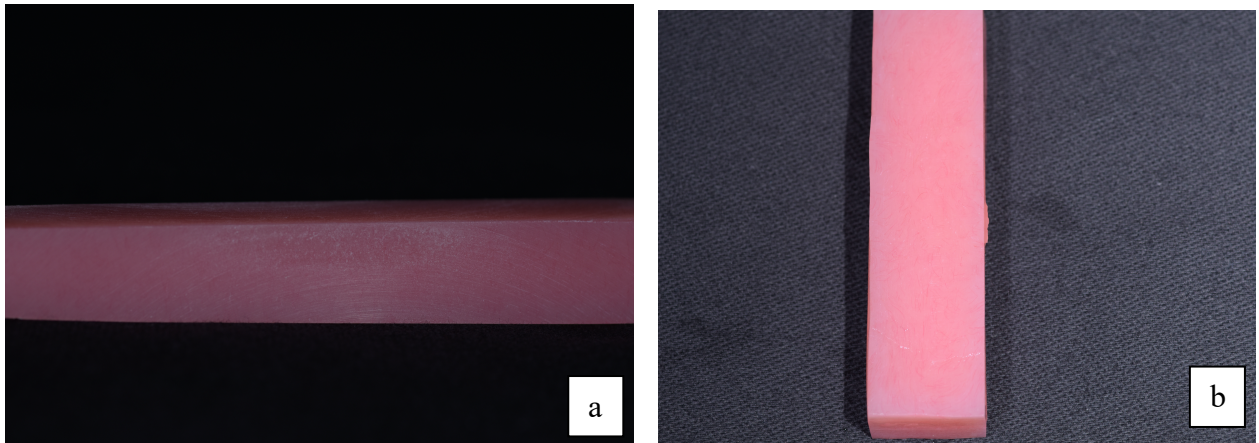


Figure 6(a), (b): Finished acrylic bars fabricated by the (C) injection molding method

3.2.2 Lucitone 199 CAD Denture Base Disc Group (M): The pre-polymerized [(98.5x35) mm] disc (Fig. 7) was cut, using a handsaw, into blocks that were further processed by grinding and polishing into NTP specimens of required dimensions.



Figure 7: Lucitone 199 CAD Disc

3.2.3 Lucitone 3D Print Denture Group (P): Autodesk Fusion 360 (San Rafael, CA), which is a cloud-based CAD software, was used to design oversized NTP of dimensions (10x10x10x40) mm (Fig. 8). The CAD was subsequently converted into a standard tessellation language (STL) file, which is the native file for the stereolithography printing (Fig. 9). The STL file was sent to Carbon M2 printer (Redwood City, CA) for the 3D printing of NTP. The orientation of the prism with respect to the build platform was 0°. The XY (2D) resolution of the printer was 75 μm (default setup by manufacturer) and Z resolution was set at 50 μm . Lucitone 3D print resin was used as tank material. The printed NTP were given a wash cycle in ethyl alcohol and post processed using a light curing unit to fully cure to final stage. These oversized NTP (Fig. 10 a and b) were further processed by grinding and polishing into NTP specimens of required dimensions.

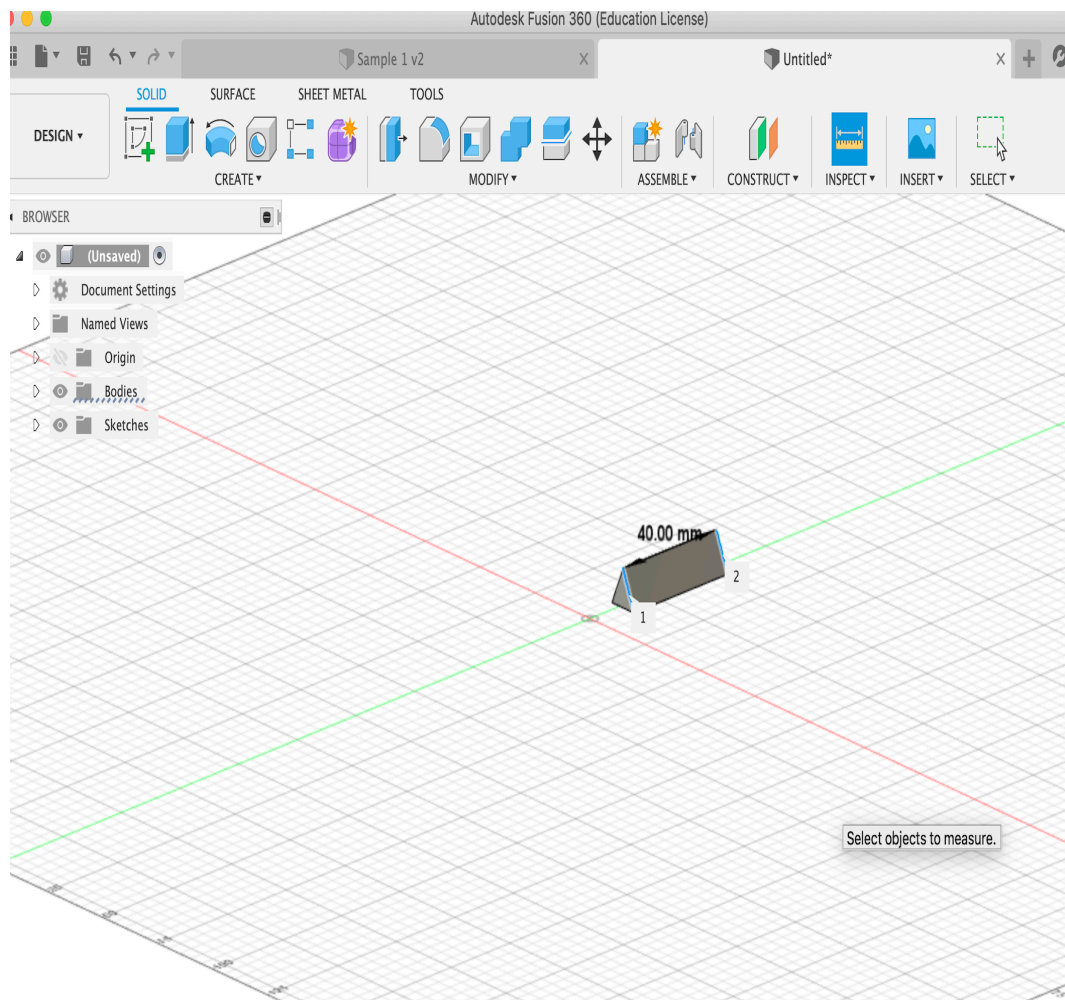


Figure 8: CAD file designed using AutoDesk Fusion 360 Software

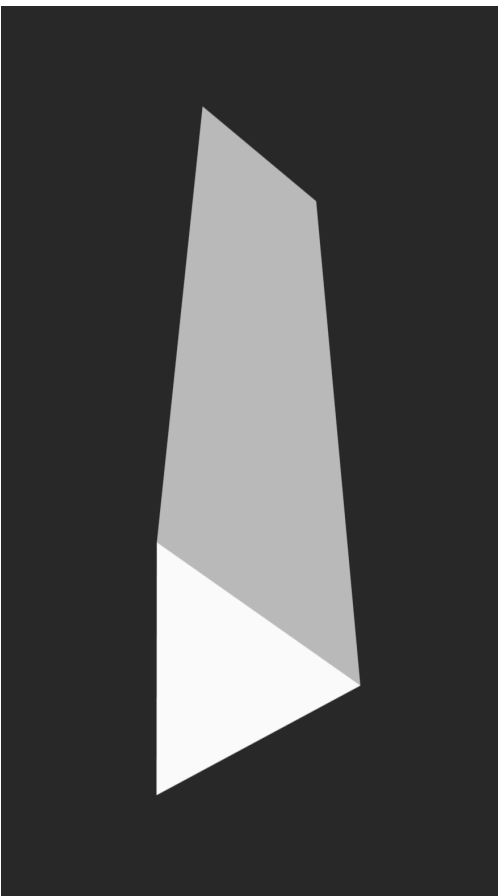


Figure 9: STL file for printed samples

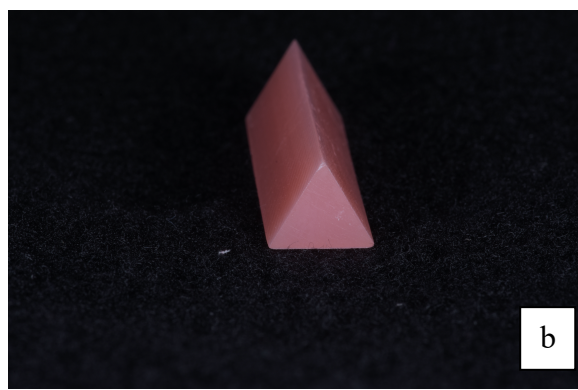


Figure 10 (a), (b): Printed triangular prisms

3.3 Sample Size Calculation

A power analysis ($\alpha = 0.05$ and $\beta = 80\%$), according to Lehr's equation (Equation 1) (Rule of Thumb) (131) was performed to determine the required sample size (n). A 20% difference between the means of two groups was considered to be clinically relevant.

$$n = \frac{16}{\Delta^2}$$
$$\Delta = \frac{\mu_0 - \mu_1}{\sigma} = \frac{\delta}{\sigma}$$

Equation 1: Lehr's Rule of Thumb

In Equation 1, Δ is the standardized difference in units of the standard deviation, is the treatment difference to be detected. The mean and standard deviation from the study by Lee et al. (35) were used in the calculation. The following values were used to calculate the sample size.

$$\text{Mean} = 1.84$$

$$\text{SD} = 0.33$$

$$\Delta = 1.12$$

The calculated sample size was $n = 13$ per group.

Denture bases are brittle material and the presence of intrinsic defects of different sizes can affect K_{IC} . Since these intrinsic defects are not normally distributed in the material and are more likely to result in material failure under a given stress, a two-parameter Weibull statistics [equation 2: (136)] was used to analyze the results.

$$P_f = 1 - \exp \left[- \left(\frac{K_{IC} - K_{IC_{II}}}{K_{IC_{\theta}}} \right)^m \right]$$

Equation 2: Two-parameter Weibull statistics

As recommended by Quinn and Quinn (136), a sample size of 20 would produce least bias in a Weibull analysis. Therefore, a sample size of $n=20$ for each test group was chosen.

3.4 K_{IC} Test

The notchless triangular prism (NTP) fracture toughness (K_{IC}) (126) test was used to determine the K_{IC} of conventional (C), CAD/Milled (M) and CAD/3D-printed (P) denture base materials.

3.5 Specimen Preparation

Forty NTP specimens [(6x6x6x12) mm] were prepared for each group.

For conventional (C) test groups, the prepared bars were polished on each side using silicon carbide abrasive disk of grit size 600 (Buehler, Lake Bluff, IL) to limit finishing/polishing at later stages. The bars were subsequently adhered using double-sided tape, to a custom fabricated jig (Fig. 11) that allow 60° angle cutting of specimen, resulting in a prism. The whole assembly was transferred to the Isomet low speed saw (Buehler, Lake Bluff, IL) and the prism specimens were cut from the bar using a diamond impregnated blade (MK Diamond Products, Inc., Torrance, USA) under constant irrigation (Fig. 12). The prisms obtained were ground, finished and polished using custom finishing/polishing jig under constant irrigation using 320/600-grit SiC paper on a Metaserv wheel grinder (Buehler, Lake Bluff, USA) to their final dimensions. For Milled (M) and Printed (P) test groups, the previously prepared triangular prisms were mounted in a custom finishing and polishing jig (Fig. 13). The samples for both these groups were finished and polished using the same methods as for the conventional test group samples, using SiC abrasive discs.

A digital caliper was used to ascertain the dimensions of the specimens at various intervals until the final dimensions were vobtained [(6x6x6x14) mm]. The length of the prism specimens was kept at 14 mm, 2 mm longer than the required length for the custom specimen testing holder. This increased length has no effect on the testing methodology. However, it allowed for proper holding of the specimen in the custom specimen holder and prevented the sample from slipping out of the holder.

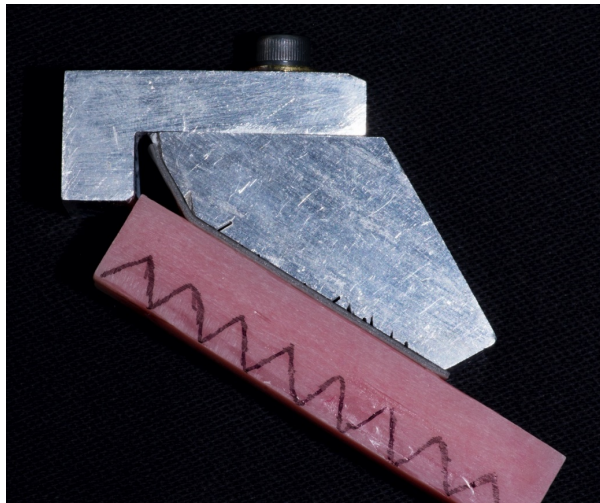


Figure 11: Custom Cutting Jig



Figure 12: Isomet saw

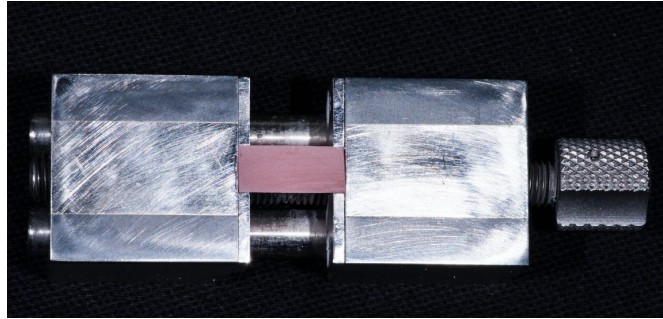


Figure 13: Custom Grinding Jig

3.6 Water storage and conditioning

The prepared 120 NTP samples were aged in a $(37 \pm 1) ^\circ\text{C}$ water bath (Isotemp Incubator Model 630D (Fisher Scientific, Ottawa, Canada) (Fig. 14). Half of the samples ($n = 20/\text{group}$) were tested after 7 d of storage and the other half ($n = 20/\text{group}$) after 90 d of storage. Prior to testing, the samples were moved to a $(23 \pm 1) ^\circ\text{C}$ water bath and conditioned for (60 ± 15) min, as per ISO 20795-1.(19)



Figure 14: Samples being aged in an Incubator

3.7 Notchless Triangular Prism (NTP) Specimen Fracture Toughness Test

Each specimen was carefully viewed under a light microscope (Olympus, Tokyo, Japan) to check for irregularities and to identify a flawless edge on which to create a crack initiation point. The prisms were secured in one half of the custom specimen holder (Fig. 15). A ~0.1 mm deep defect, to act as a crack initiation point, was introduced on the flawless edge using a 200 μm thick surgical GEM stainless-steel blade (Ted Pella Inc., Redding, CA) and verified under 6X optical magnification. The side opposing the initiated defect was marked using a sharpie point to identify the direction of crack propagation, later to be used for fractographic analysis under scanning electron microscope. A custom mounting jig was used to secure the two halves together, utilizing a 200 μm thick spacer that kept the two halves of the specimen holder apart, replicating the CNSR specimen configuration [Fig 16 (a),(b)].

The test assembly was secured in custom designed grips, attached to an Instron 4301 (Instron; Canton, MA), equipped with a 1 kN Instron load cell and controlled by Bluehill 2 software (Instron, Norwood, USA) (Fig. 17). The test assembly was loaded in tension at a crosshead speed of 0.1 mm/min until crack arrest or failure. The maximum recorded load was used to calculate K_{IC} , using the equation below:(126)

$$K_{IC} = Y_{min}^* \frac{P_{max}}{DW^{1/2}}$$

Equation 3: Calculation of K_{IC}

In Equation 3, Y_{min}^* = minimum value of the dimensionless stress intensity factor coefficient (28 for the NTP test), D = specimen diameter (12 mm), and W = specimen length (10.4 mm).

Bubsey et al. reported the Y^*_{min} value for specimens in which length/diameter (W/D) ratio was between 1.5 to 2 and the initial crack length (a_0) to specimen length (W) ratio (α_0) was in range of 0.2-0.5.(137) In NTP testing, α_0 is 0.5 and the W/D ratio is 0.88. Since ratio of W/D is outside the range reported by Bubsey et al., Ruse et al. extrapolated and calculated the value of Y^*_{min} to be 28 for the NTP testing.(126)(137)

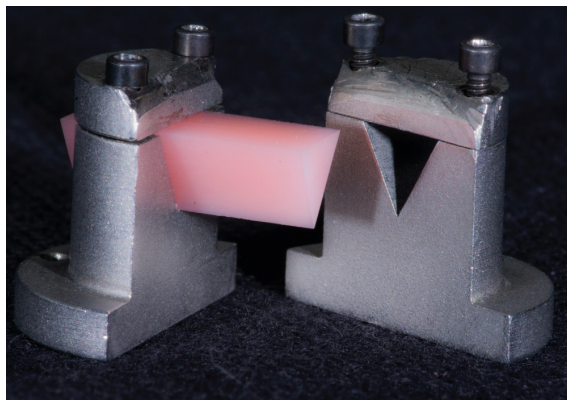


Figure 15: NTP specimen custom holder

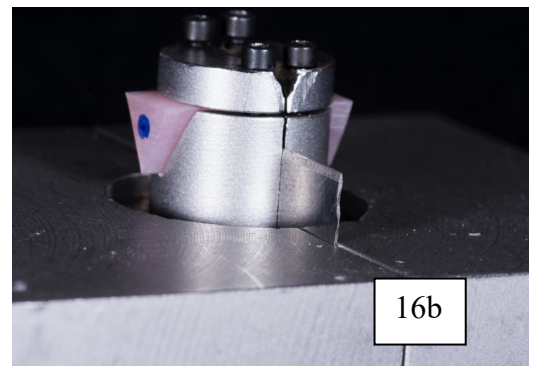
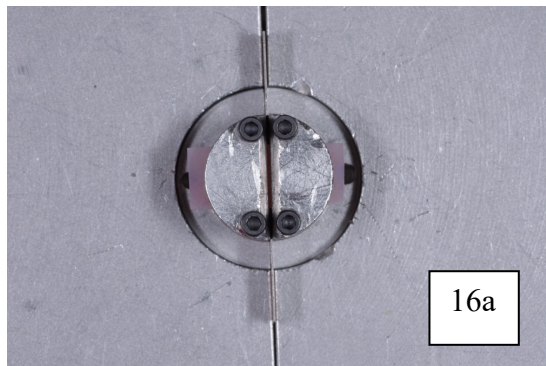


Figure 16 (a), (b): Custom Mounting Jig

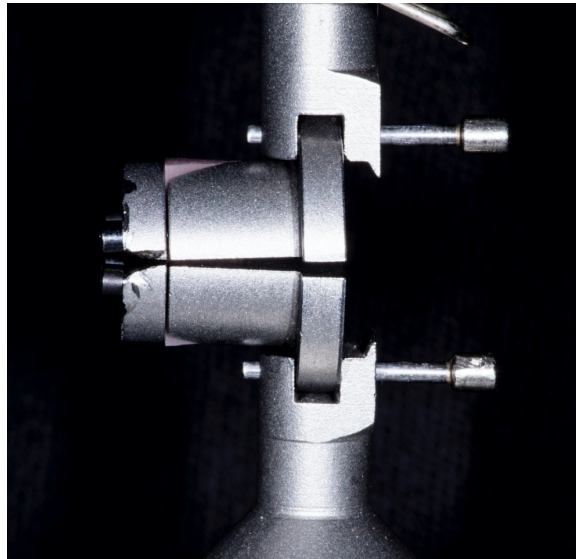


Figure 17: Test Assembly

3.8 Statistical Analysis

The collected K_{IC} data was assessed for normality and analyzed by two-way ANOVA followed by Scheffé multiple mean comparisons ($\alpha = 0.05$) (SPSS v27 software; IBM, Armonk, NY). For between mean comparisons at 7 d and 90 d, independent student t-tests were performed. Weibull statistics was also used to analyze the results, to determine the characteristic Weibull K_{IC} and the Weibull modulus (m). The equation 4 below, results in the graphical representation of these Weibull parameters.

$$\ln \left[\ln \left(\frac{1}{1 - P_f} \right) \right] = m \ln \sigma - m \ln \sigma_\theta$$

Equation 4: Weibull formula

The analysis of these graphs provides us with the parameters attributed to different tested material. The slope of the linear trend line provides us the Weibull modulus (m), which indicates the

reliability of the tested material. The steeper the slope, the higher the Weibull modulus (m) and the higher is the reliability of the tested material. Characteristic Weibull value (K_{IC}) was determined as the value corresponding to the failure probability value $P_f = 63.2\%$.

3.9 Scanning Electron Microscopy

Since crack arrest was recorded for all test specimens, they were broken into halves by hand for fractographic analysis. The two halves of all fractured samples were examined under a light microscope to characterize the site of crack initiation, surface texture, presence/absence of defects and failure mode. One representative sample from each test group was selected (closest to the mean K_{IC}) for fractographic analysis with a scanning electron microscope (SEM) (Hitachi, S-3000N; Hitachi, Japan). Samples were mounted on SEM studs and coated with gold in an Edwards S150A sputter coater (Edwards Vacuum; Crawley, UK). Photomicrographs were recorded for each half at various magnifications (25x, 150x, 500x).

Chapter 4: Results

4.1 Fracture Toughness (K_{IC})

Twenty samples from each group were tested at both 7 d and 90 d, meeting the minimum sample size requirement for performing Weibull statistics. For each test group and storage time, the results are summarized in the Table 8 and presented as Box plots in Fig. 18:

Table 8: Results (Mean \pm SD)[#]

Material Group	K_{IC} (MPa·m ^{1/2})	
	7 d	90 d
Lucitone 199 Denture base resin (C)	2.09 \pm 0.13 ^{b*}	1.82 \pm 0.19 ^{b*}
Lucitone 199 CAD (M)	1.96 \pm 0.14 ^{b*}	1.59 \pm 0.27 ^{c*}
Lucitone Digital Print (P)	2.23 \pm 0.11 ^a	2.24 \pm 0.17 ^a

[#] Identical small letter superscript identifies no significant differences between the test groups at the same storage time;

Asterisks identify significant differences between 7 d and 90 d groups.

The box plots show the median, minimum and maximum range of K_{IC} for each test group after 7 d and 90 d (Fig. 18). The plots show that P groups have higher K_{IC} than C and M groups. Wider distributions were noted in all the test groups after 90 d storage in 37 °C water.

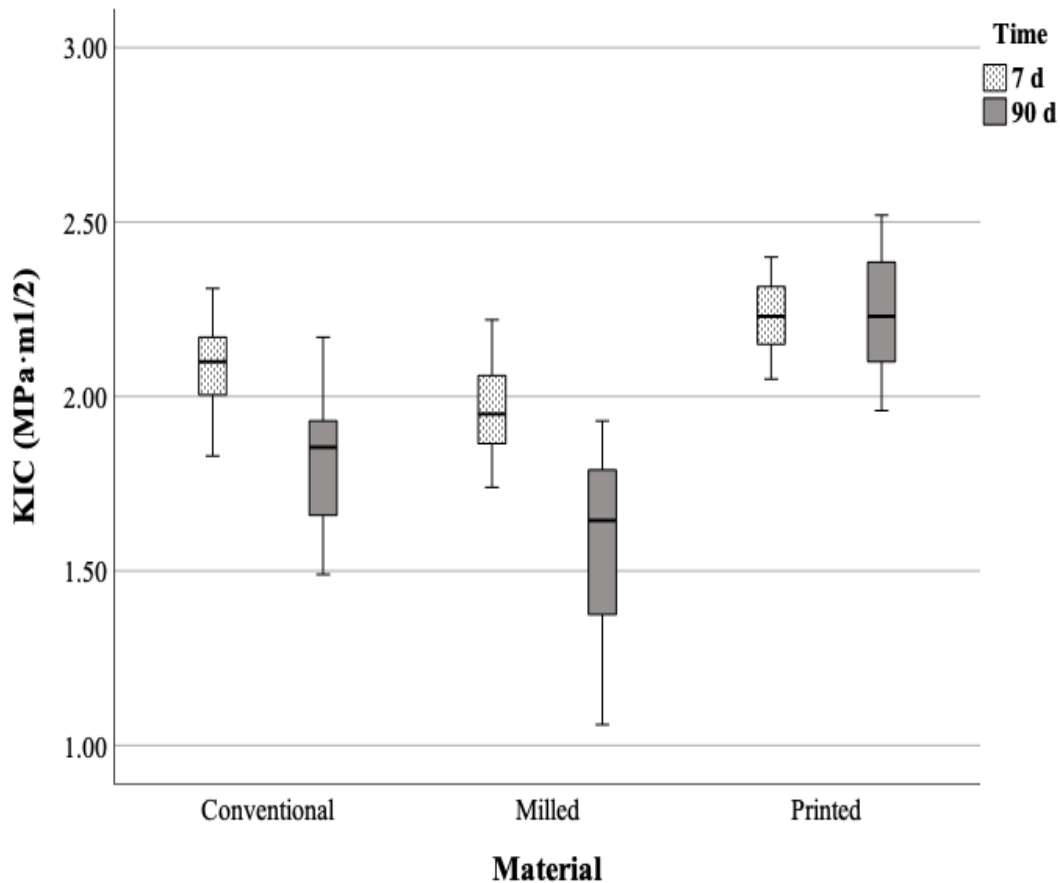


Figure 18: Box Plot

Analysis of the results by two-way ANOVA followed by Scheffé post hoc tests, showed that the three tested materials had significantly different K_{IC} at both 7 d (Fig. 19) and 90 d (Fig. 20), with the same ranking, i.e., P > C > M ($p < 0.005$).

Independent student t-test for between mean comparisons at 7 d and 90 d, have shown that ageing in 37 °C water for 90 d resulted in a significant decrease in K_{IC} in the C and M groups ($p < 0.001$).

Multiple Comparisons

Dependent Variable: KIC_final
Scheffe

(I) Material	(J) Material	Mean Difference (I-J)	Std. Error	Sig.	95% Confidence Interval	
					Lower Bound	Upper Bound
Conventional	Milled	.1255*	.03958	.010	.0260	.2250
	Printed	-.1380*	.03958	.004	-.2375	-.0385
Milled	Conventional	-.1255*	.03958	.010	-.2250	-.0260
	Printed	-.2635*	.03958	.000	-.3630	-.1640
Printed	Conventional	.1380*	.03958	.004	.0385	.2375
	Milled	.2635*	.03958	.000	.1640	.3630

Based on observed means.

The error term is Mean Square(Error) = .016.

*. The mean difference is significant at the .05 level.

Figure 19: Scheffé post hoc K_{IC} 7 d

Multiple Comparisons

Dependent Variable: KIC_final
Scheffe

(I) Material	(J) Material	Mean Difference (I-J)	Std. Error	Sig.	95% Confidence Interval	
					Lower Bound	Upper Bound
Conventional	Milled	.2315*	.06791	.005	.0608	.4022
	Printed	-.4150*	.06791	.000	-.5857	-.2443
Milled	Conventional	-.2315*	.06791	.005	-.4022	-.0608
	Printed	-.6465*	.06791	.000	-.8172	-.4758
Printed	Conventional	.4150*	.06791	.000	.2443	.5857
	Milled	.6465*	.06791	.000	.4758	.8172

Based on observed means.

The error term is Mean Square(Error) = .046.

*. The mean difference is significant at the .05 level.

Figure 20: Scheffé post hoc K_{IC} 90 d

4.2 Crack Propagation and Arrest

Fig. 21, 23 and 25 show representative 7 d and 90 d load-displacement curves for specimens in groups C, M, and P, respectively. The curves of groups C (Fig. 21) and M (Fig 23) look similar to each other, with the 7 d slopes being much steeper than the 90 d ones. The 7 d and 90 d slopes of the P group (Fig. 25) are similar to each other and look similar to the 90 d C and M curves. Upon examination of the 7 d and 90 d cracked surfaces under a high-resolution macro lens, a smooth fracture was noticed for C (Fig. 22) and M (Fig. 24) denture base specimens, with crack arrest. No permanent deformation was seen in the specimens and the morphology was indicative of brittle fracture. Calibrated analyses of the cracked surfaces showed that the crack propagated much farther (4.38 mm) in 7 d specimens (Fig. 22 a) compared to at the 90 d specimens (3.43 mm) (Fig. 22 b) C group. Similar results were seen for the M group (Fig 25 a and b), with crack arrest occurring much farther (3.81 mm) at 7 d than at 90 d (3.34 mm). Distinct failure zones in the C and M groups are seen as shown by pointed arrows in the Figs 22 a, b and 24 a, b.

The highest load values were recorded in P group (Fig. 25), followed by C group, and M group displaying the lowest values. The 7 d P group showed a distinct load-displacement behavior: increase in load up to ~ 100 N, followed by a plateau stage where minimal changes in load occurred with changes in displacement. Once sufficient energy was absorbed, the plateau was followed by a subsequent increase in load before a sudden drop, corresponding to failure by crack arrest (Fig. 25). The 90 d P specimens did not exhibit this behavior.

Both 7 d and 90 d P specimens showed crazing (broken double arrows), with a teardrop pattern at the crack tip before the arrest occurred (pointed arrows) (Figs. 26 a and b). There was also large permanent plastic deformation visible in these specimens. Two distinct teardrop patterns were seen

in the 7 d specimen while only a single teardrop was seen in 90 d; both were followed by a zone of crazing. Another interesting finding was that the zone of crazing was much larger in the 90 d specimens than in the 7 d specimens. However, the crack arrest in both 7 d and 90 d specimens occurred at similar distances (4.19 mm and 4.21 mm).

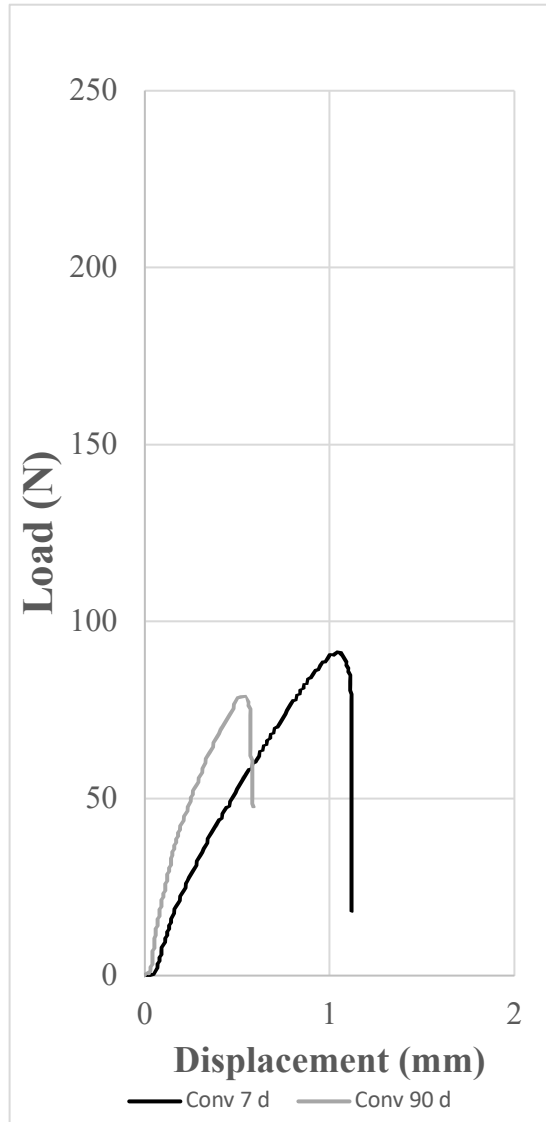


Figure 21: Load/Displacement graph for C group at 7 d and 90 d

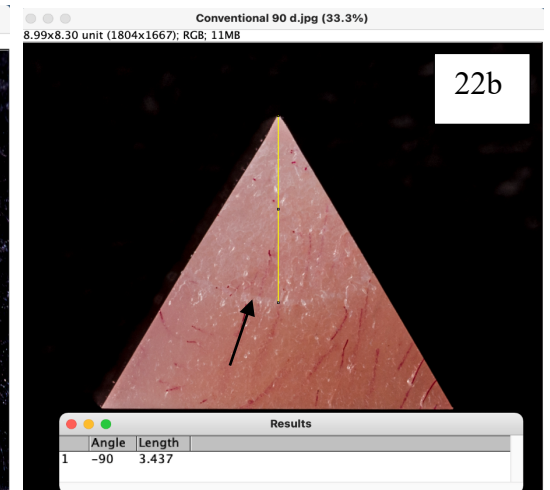
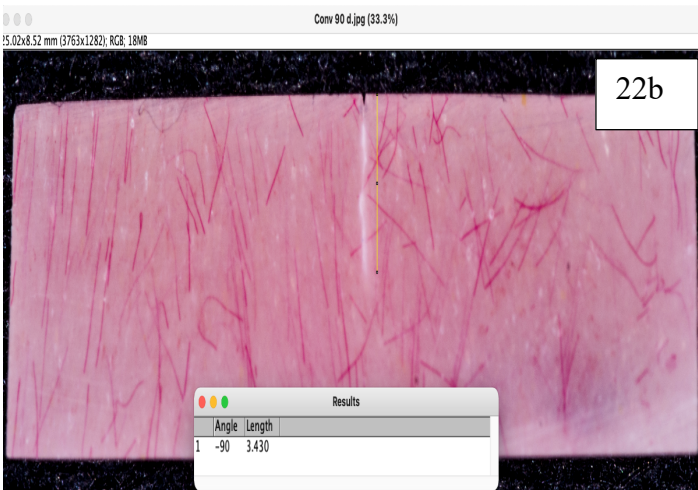
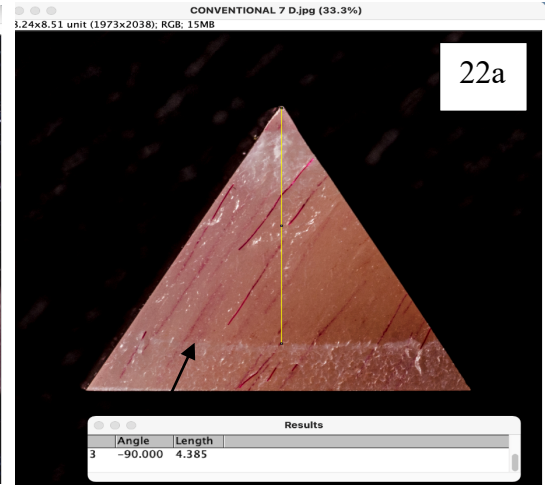
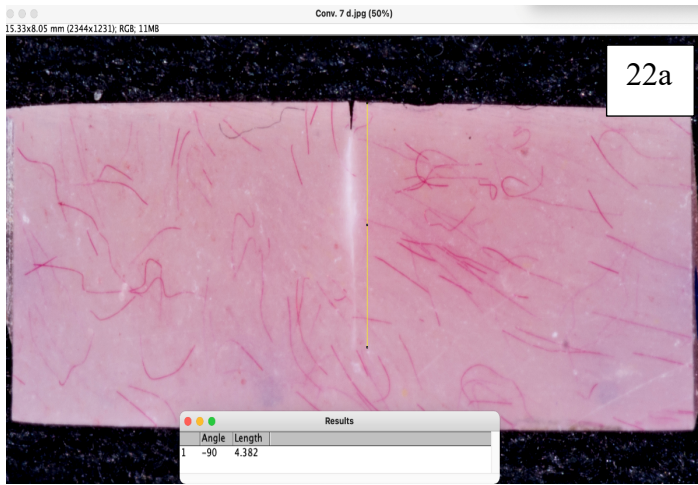


Figure 22 (a), (b): Crack Propagation and arrest in C specimens at 7 d and 90 d

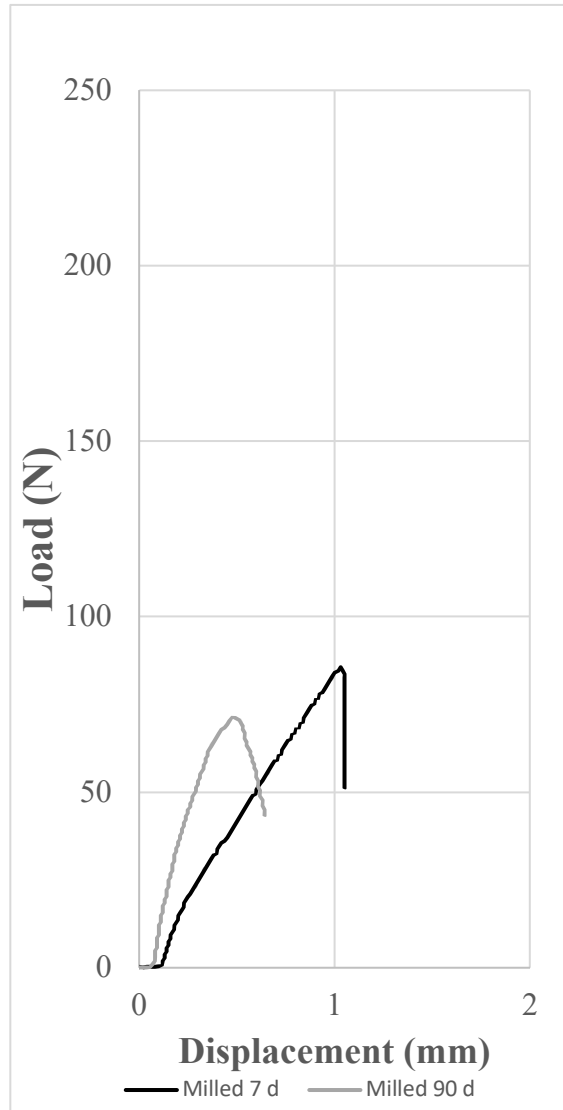


Figure 23: Load/Displacement graph for M group at 7 d and 90 d

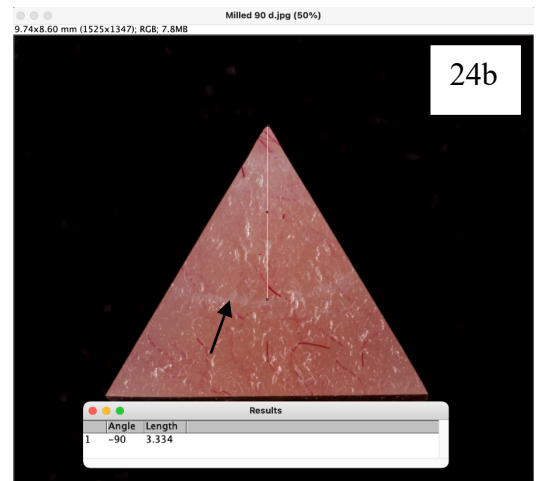
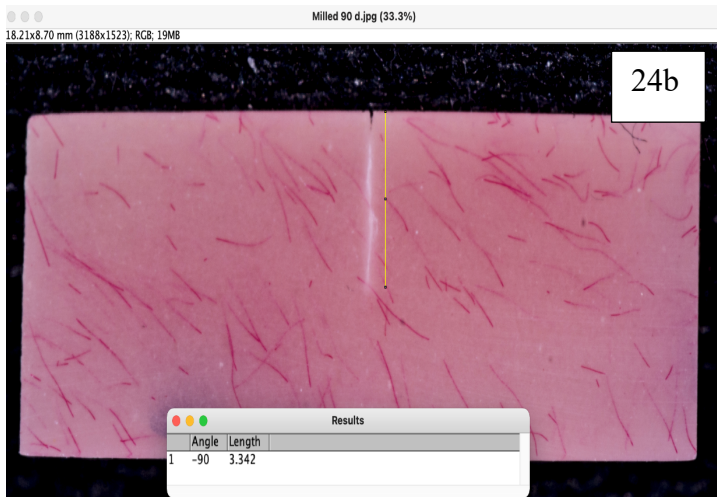
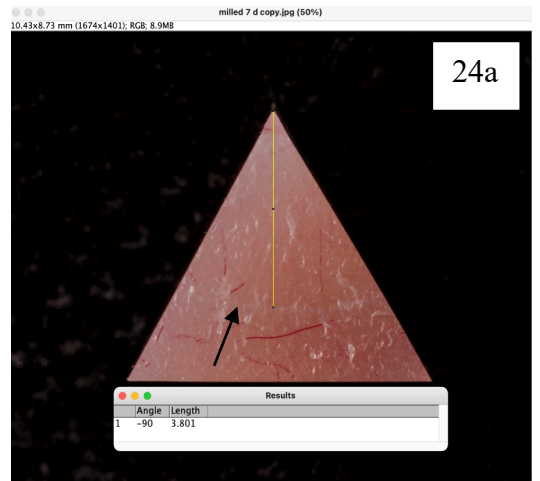


Figure 24 (a), (b): Crack Propagation and arrest in M specimens at 7 d and 90

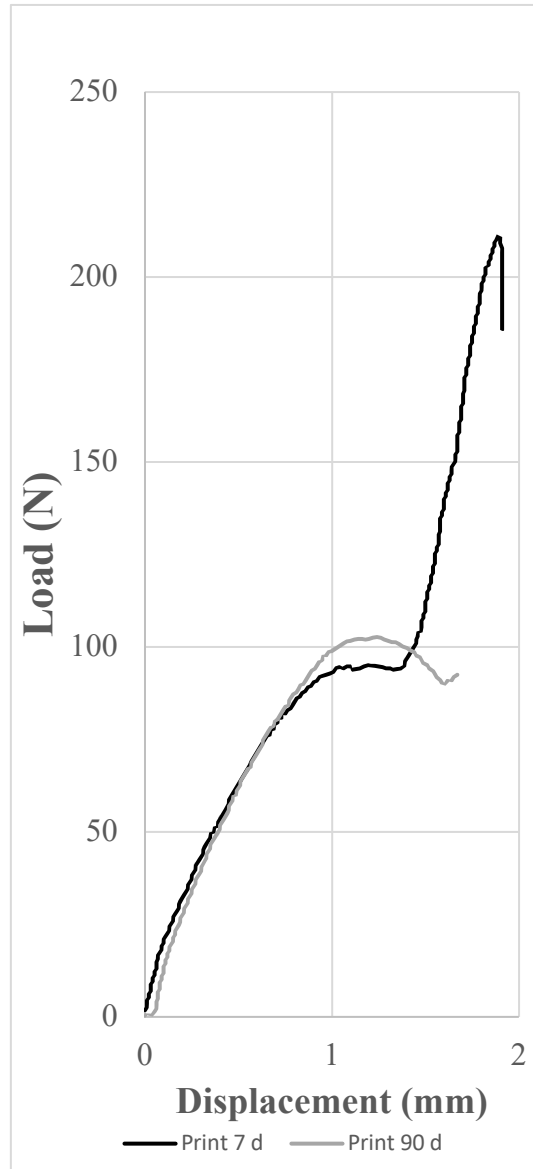


Figure 25: Load/Displacement graph for P group at 7 d and 90 d

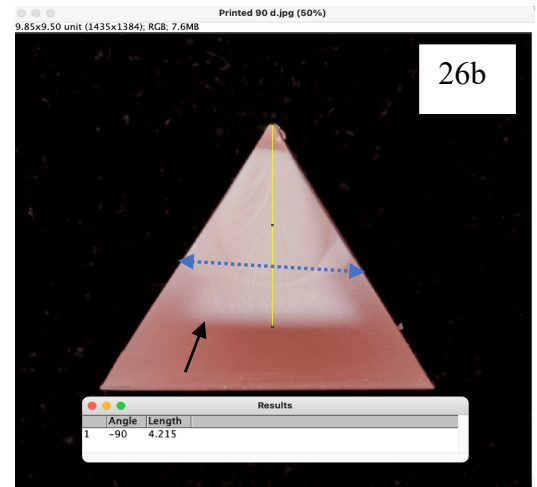
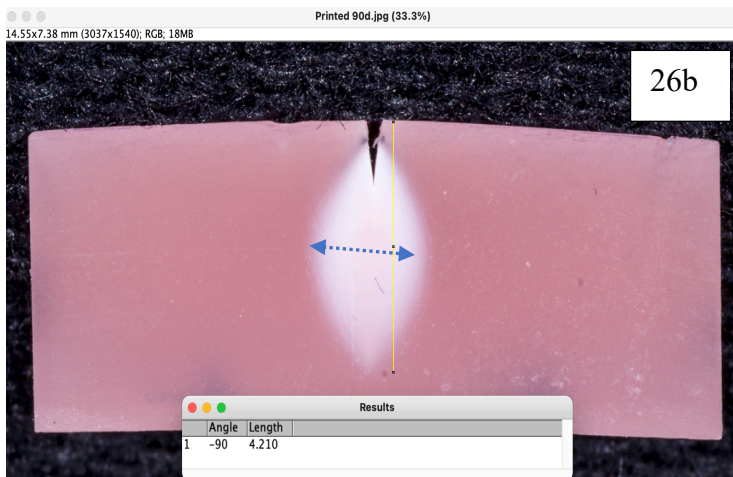
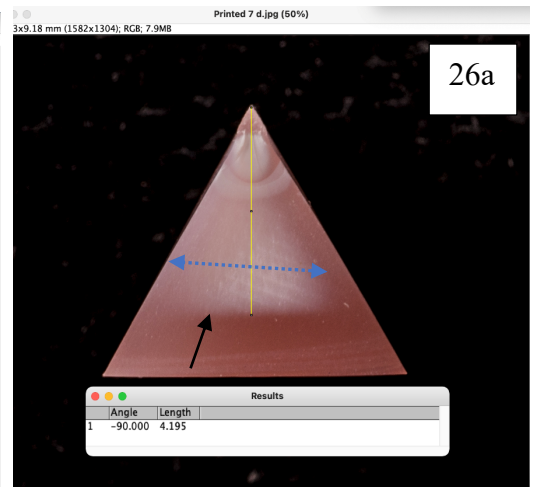
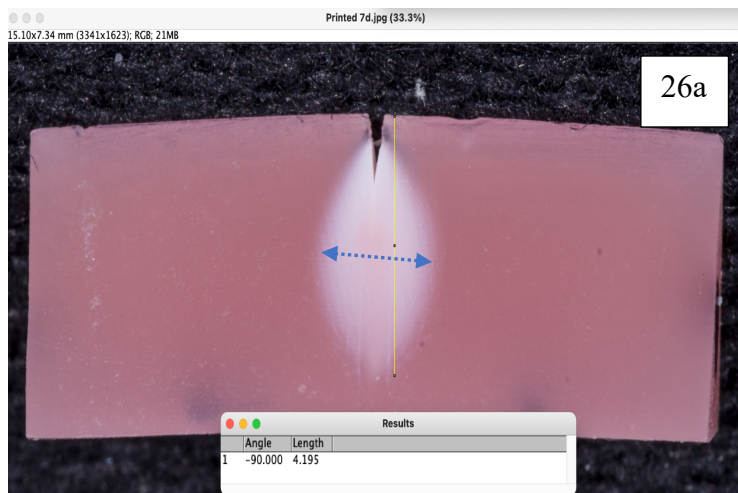


Figure 26 (a), (b): Crack Propagation and arrest in P specimens at 7 d and 90 d

4.3 Work of Fracture

Work of fracture (WOF) is the work per unit area, i.e., the total energy required for crack propagation divided by the cross-sectional area of the crack.

Table 9 summarizes the WOF for the specimen groups and was determined by calculating the area under the load displacement graphs (in J) (Figs. 21, 23, 25) and dividing it by twice the cross sectional area (in m²) of the fractured surfaces [Figs. 22, 24, 26 (b)].

$$\text{WOF} = U / 2SA$$

Equation 5: Calculation of WOF

Where U = energy (in J) calculated from the area under the load displacement curves,

SA = surface area (in m²) of the fractured surfaces.

Table 9: Work of Fracture (WOF) (in KJ/m²)

Material (Group)	WOF (in KJ/m ²)	
	7 d	90 d
Lucitone 199 Denture base resin (C)	~ 2.3	~ 1.7
Lucitone 199 CAD (M)	~ 2.7	~ 1.8
Lucitone Digital Print (P)	~ 8.7	~ 6.3

4.4 SEM Analysis

Figs. 27-32 show SEM images recorded under 25x and 150x magnification, revealing various zones on the fractured surfaces: the zone of crack initiation and slow crack propagation, followed by the zone of rapid crack propagation, clearly discernable at 150x magnification and marked on the figures.

The zone of crack initiation was marked by the presence of vertical striations on the surface, and it was present in all groups. The immediate relatively smooth zone, from where cracks radiate outwards from the flaw (crack initiation), was the zone of slow crack propagation, also called the mirror. Immediately following the mirror, the presence of hackle lines marks the area of rapid crack propagation. The materials underwent crack propagation and ultimately crack arrest, distinct from the hackle lines. The crack arrest was well defined for 7 d C and P groups, but not for the others.

All specimens, except for the 7 d P specimen group, showed single “mirror” immediately adjacent to the crack initiation. Two zones of slow crack propagation were seen in the 7 d P specimen, one immediate to the crack initiation and one after the initial rapid crack propagation has occurred. The zone of slow crack propagation was clearly seen as a plateau on the load displacement graph (Fig. 25 pg. 58), after an initial rapid crack propagation zone.

The hackle lines for the C and M specimen group were similar to those seen in brittle material fracture. For the P specimen group, circular cracks radiate outward from the flaw, with the advancing crack front creating hyperbolic markings on the fractured surface, similar to those seen in polymers.

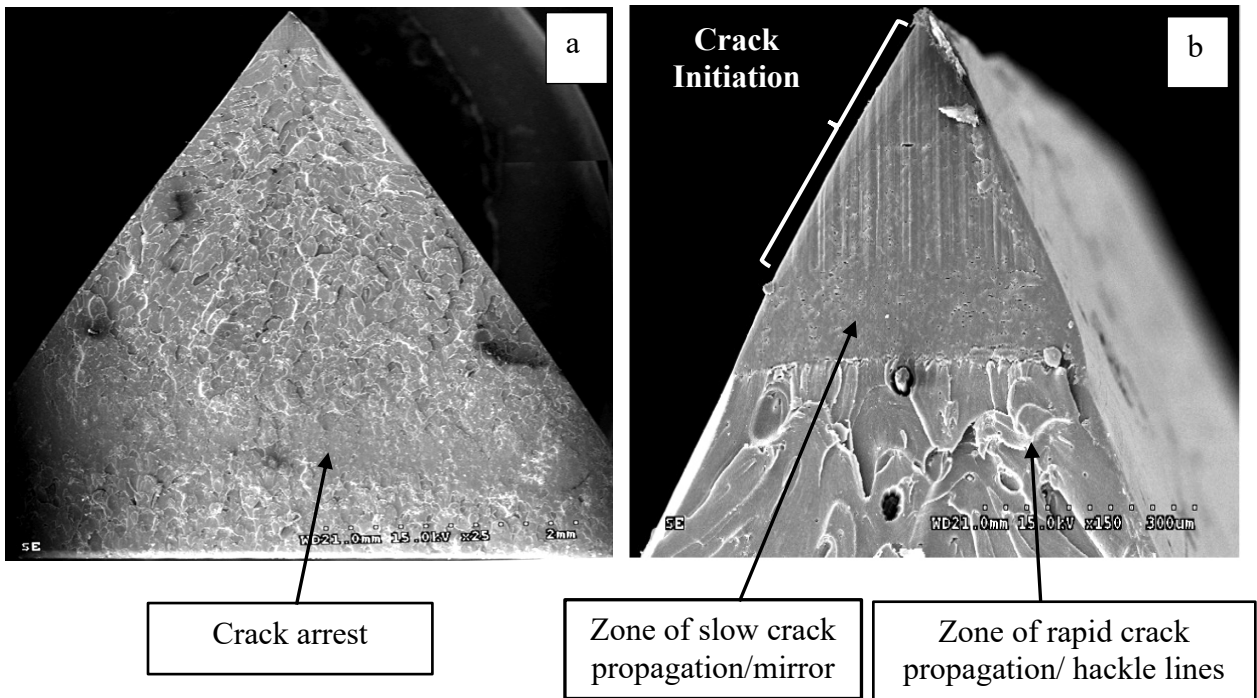


Figure 27 (a), (b): SEM images - C 7 d at 25x (a) and 150x (b) magnification

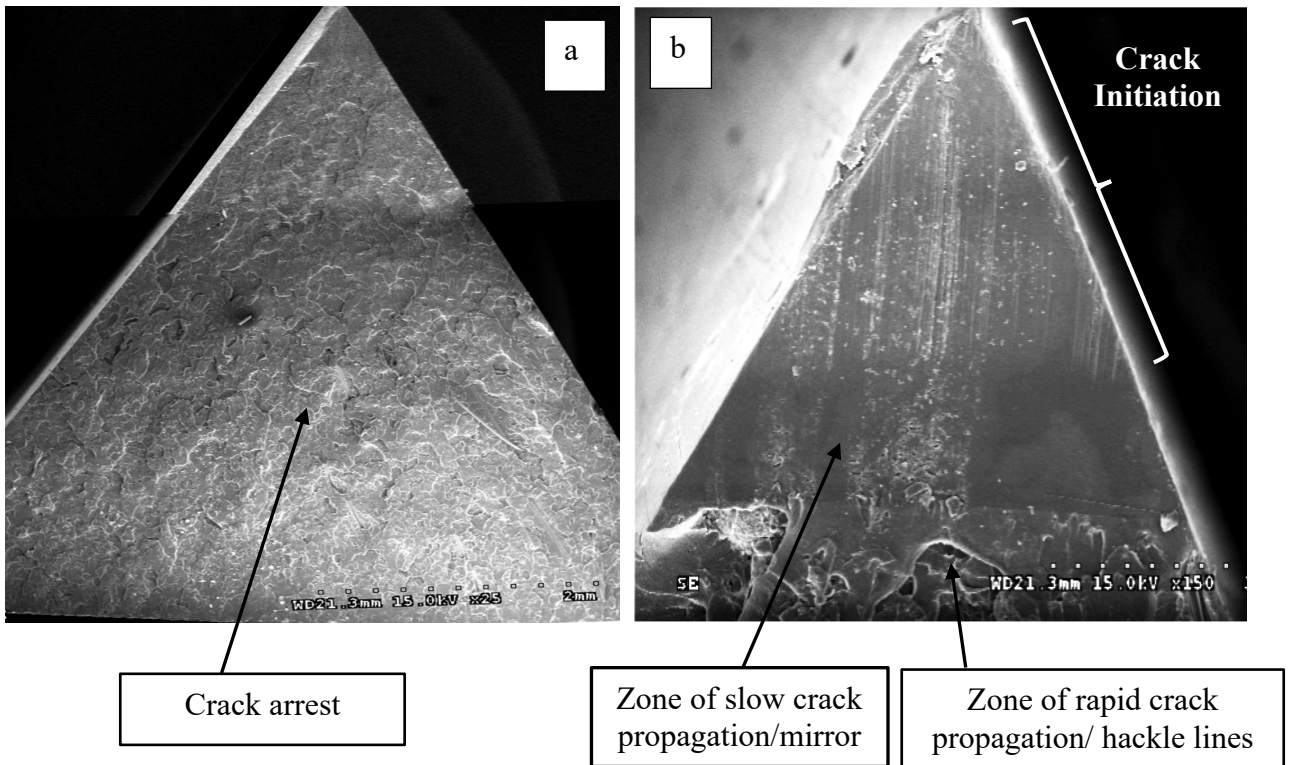


Figure 28 (a), (b): SEM images - C 90 d at 25x (a) and 150x (b) magnification

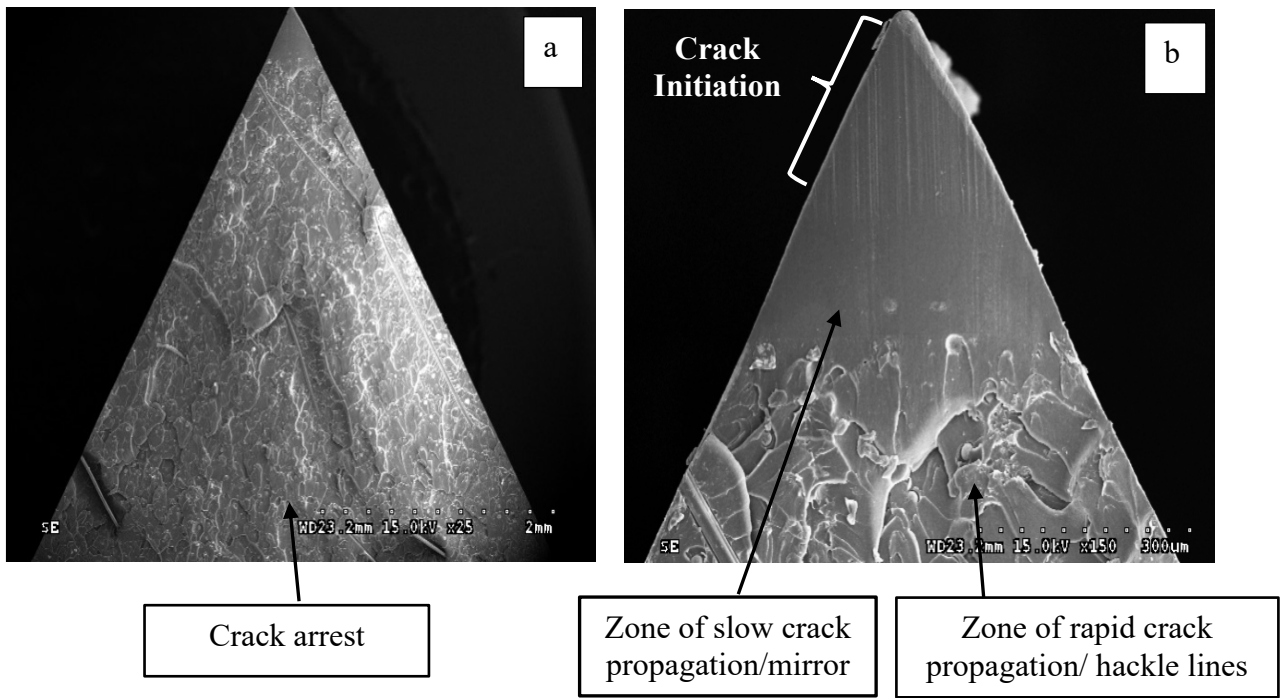


Figure 29 (a), (b): SEM images - M 7 d at 25x (a) and 150x (b) magnification

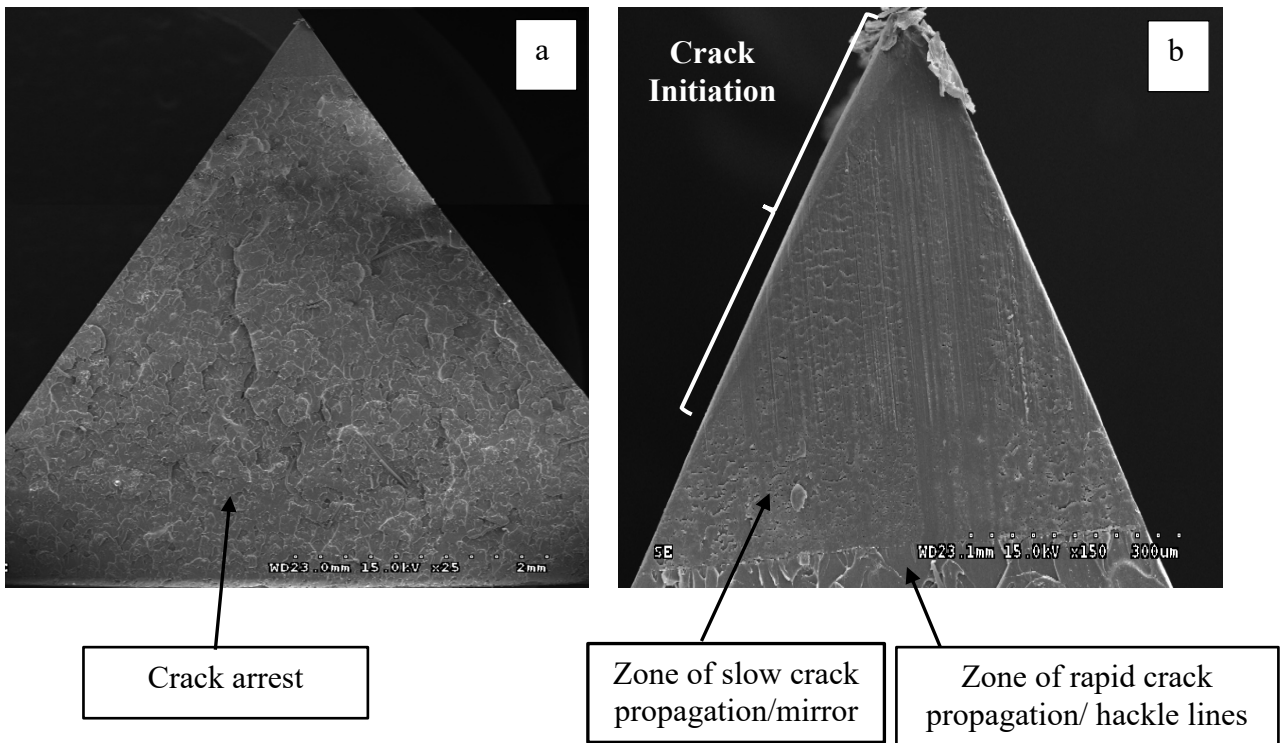


Figure 30 (a), (b): SEM images - M 90 d at 25x (a) and 150x (b) magnification

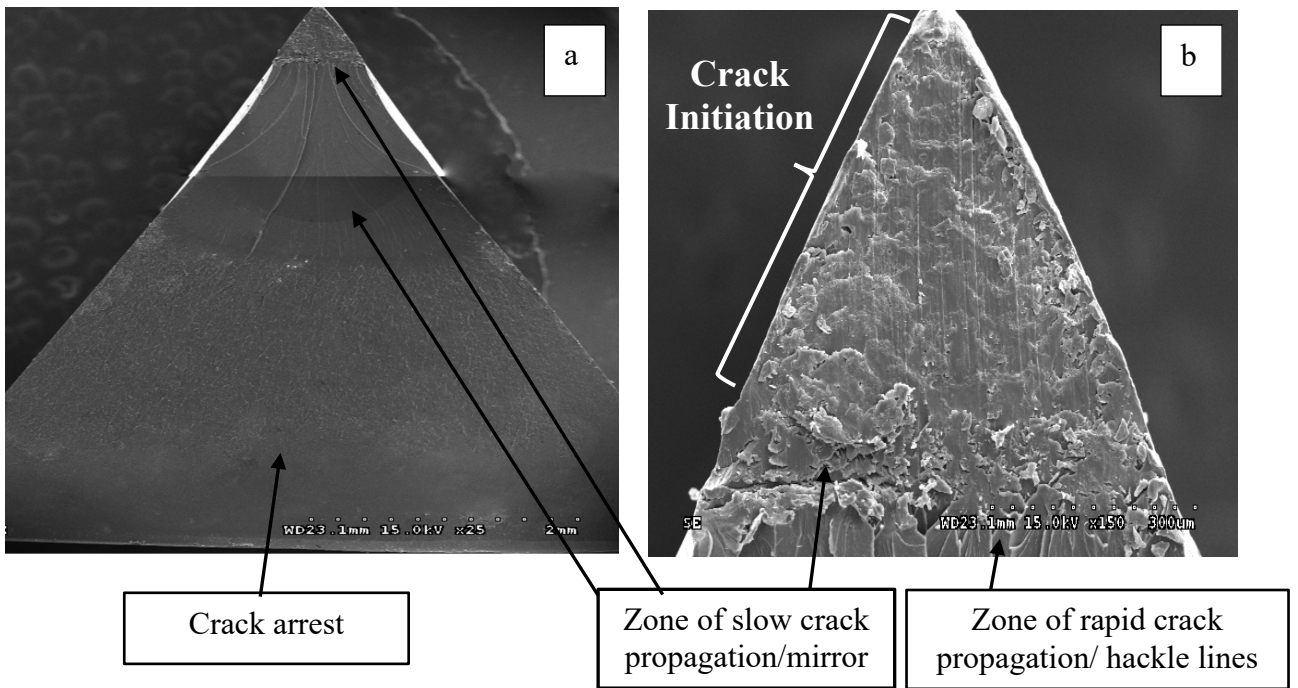


Figure 31(a), (b): SEM images - P 7 d at 25x (a) and 150x (b) magnification

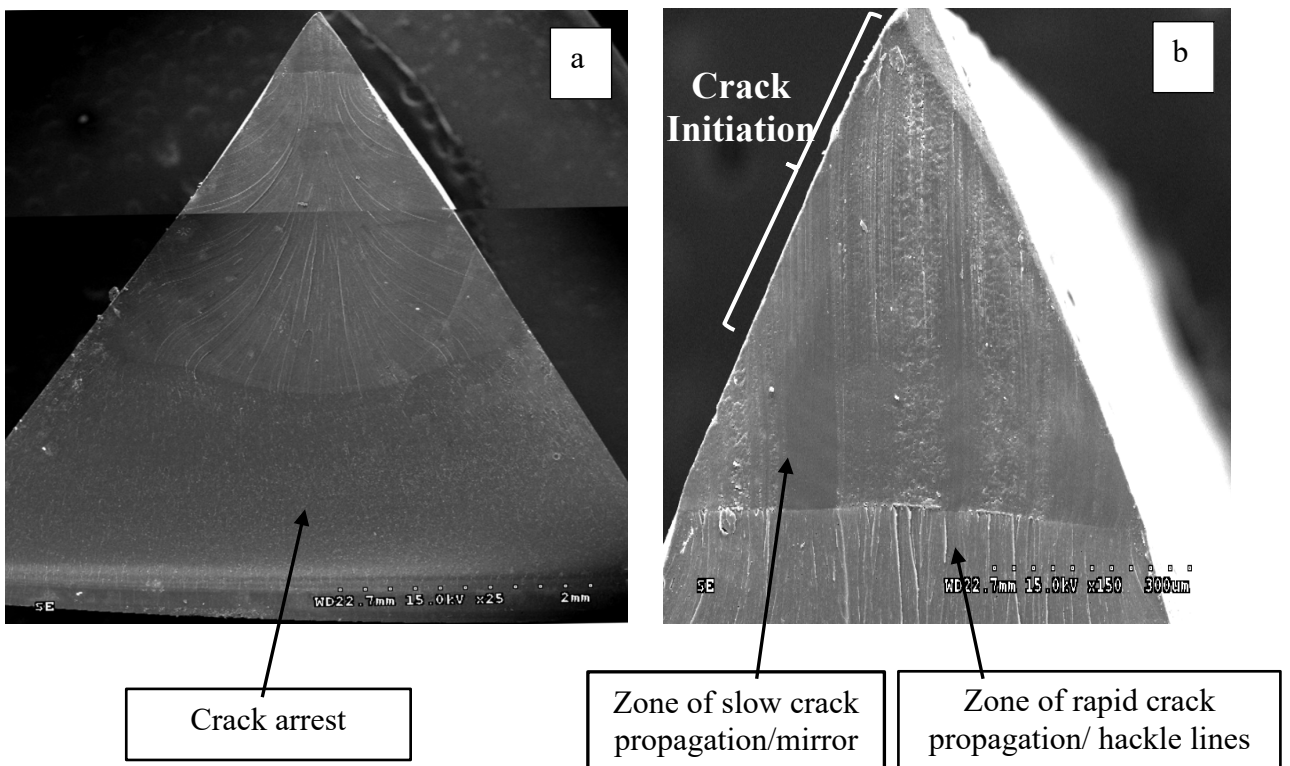


Figure 32 (a), (b): SEM images - P 90 d at 25x (a) and 150x (b) magnification

4.5 Weibull Statistics

Table 10 summarizes the results of the Weibull statistics analysis while Fig. 33 shows the Weibull plots.

Table 10: Weibull Modulus (m) and Characteristics Weibull Fracture Toughness (K_{IC})

Material Group	m		K_{IC} (MPa·m ^{1/2})	
	7 d	90 d	7 d	90 d
Lucitone 199 Denture base resin (C)	19.81	11.38	2.14	1.90
Lucitone 199 CAD (M)	17.01	6.58	2.02	1.71
Lucitone Digital Print (P)	23.94	16.01	2.28	2.31

From the Table 9, it should be noted that at 7 d, P group showed the highest reliability ($m = 23.94$) while the C ($m = 19.81$) and M ($m = 17.01$) groups had similar reliabilities. At 90 d, the Weibull modulus (m) of all the three groups was lower compared to that at 7 d, with M ($m = 6.58$) group exhibiting lower reliability than C ($m = 11.38$) and P ($m = 16.01$) groups. Overall, M group had the lowest reliability at both 7 d and 90 d.

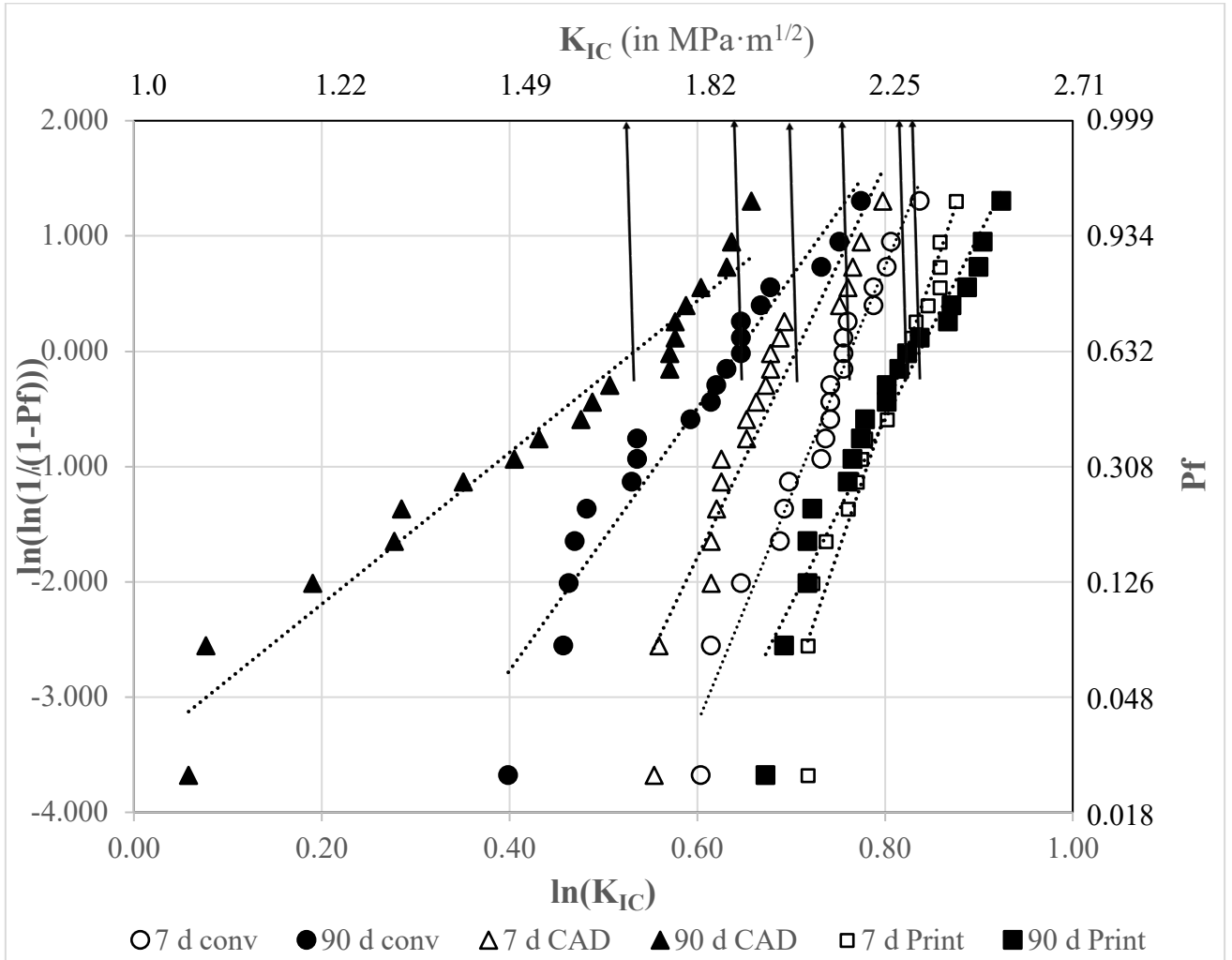


Figure 33: Weibull Plots for the tested materials

Chapter 5: Discussion

The results of this study showed significant difference in K_{IC} between C, M and P denture bases at 7 d and 90 d, thus rejecting the null hypothesis (H_{01}).

The results obtained for the C group, Lucitone 199, are in accordance with those reported by previous studies.(35)(36) A study by Pacquet et al. reported similar K_{IC} values [(2.11 ± 0.29) MPa·m^{1/2}] for milled denture base to our study.(138) As far as these authors know, there are no published results for the K_{IC} of printed denture base materials.

The C and M groups showed similar K_{IC} . The loading pattern occurred similarly in both groups, with the load increasing continuously up to the point where the specimens failed with crack arrest (Fig. 21 and 23). The characterization of the tested C and M specimens under the light microscope revealed a fine fracture line on the surface of the specimens up to the point of crack arrest and no permanent deformation of the specimens was noted (Fig. 22 and 24). The distance from the crack initiation to the crack arrest/failure was much greater at 7 d compared to 90 d in both C and M groups (Figs. 22 a, b and 24 a, b). This can explain the failure occurring at lower loads and therefore lower K_{IC} values at 90 d compared to 7 d in C and M groups.

In the 7 d P group, however, the load increased continuously up to ~100 N, at which stage, rather than decreasing sharply, it only dropped slightly, was followed by a plateau, then by an increase and finally by a sharp drop (Fig. 25). The characterization of the tested specimens under the light and scanning electron microscope revealed a significant crazing zone around the propagating crack, up to the crack arrest point (Figs. 26, 31 a). It is likely that at the site of crazing, microcrack bridging took place, allowing the load to be transmitted to the rest of the material, thus creating a

crack resistance zone. The plateau may be the area shown by a teardrop (Fig. 26 a) where significant resistance is offered by the material to the crack propagation (also seen on SEM Fig. 31(a); “mirror” area). Additional energy was absorbed by the material without any changes in load. Once the amount of energy was sufficient to overcome this zone, the material started to take more load before crack arrest occurred. We reported the K_{IC} of this group based on the highest load recorded prior to the plateau $[(2.23 \pm 0.11) \text{ MPa}\cdot\text{m}^{1/2}]$. However, if the maximum load recorded during the testing were to have been considered as a point of crack initiation/propagation, K_{IC} would have been $[(4.04 \pm 0.51) \text{ MPa}\cdot\text{m}^{1/2}]$, which is significantly higher than that of the other groups. Moreover, the area under the load displacement curve for this group, which represents the energy (in J) absorbed by the material during testing, was significantly higher in 7 d P group ($\sim 8.7 \text{ KJ/m}^2$) than that of any other groups tested. (Table 9, pg. 59)

In contrast, the plateau was not seen in 90 d P group (Fig. 25), even though the crazing around the propagating crack was still present, as was the plastic deformation of the samples (Fig 26 b). The teardrop pattern was also seen in the 90 d specimen, much closer to the area of crack arrest as compared with the 7 d P specimen. The absence of the plateau in the load displacement graph and the presence of zone of resistance (teardrop) closer to the crack arrest indicate that less resistance was offered by the material to crack propagation. The maximum recorded K_{IC} in 90 d was $[(2.24 \pm 0.17) \text{ MPa}\cdot\text{m}^{1/2}]$ and the energy absorbed by the 90 d specimen was $\sim 6.3 \text{ KJ/m}^2$. The difference in the behaviour between the 7 d and 90 d samples could be due to monomer/component leaching or polymer degradation.

Experimentally, in mode I loading, it has been determined that the ratio of plastic zone to the specimen thickness has to be ~ 0.025 in order to ensure plain strain conditions. This implies that the specimen thickness (B) and crack size (a) of the specimen has to be equal or greater than 2.5

times the square of the fracture toughness (K_{IC}) to yield stress (σ_y) ratio, as described in the following equation:(139)

$$a, B \geq 2.5 \left(\frac{K_{IC}}{\sigma_y} \right)^2$$

Equation 6: Requirement to ensure plane strain conditions

Based on the available reported values for K_{IC} and σ_y of conventional and milled denture base materials, the NTP specimen dimensions [(6X6X6x12) mm] used in this study satisfy the above requirement. In view of the significant plastic deformation and crazing observed for the printed denture base material tested, it is possible that the specimen dimensions were inadequate to secure plain strain conditions. Due to the lack of data regarding K_{IC} and σ_y of the printed denture bases, we could not determine the required sample dimensions to ensure plain strain conditions. Therefore, the K_{IC} values reported for printed denture base should be considered tentative.

The difference in crack propagation between the C or M and the P group could be due to the material chemistry and the degree of cross-linking within the polymers. Highly cross-linked polymers would exhibit significantly less crazing and plastic deformation. Urethanes form lightly cross-linked thermoset polymers, with flexible and rubbery characteristics, being more flexible than the methacrylates over wide temperature ranges. Urethane methacrylate is the main component in P denture bases, while C and M denture bases are based on polymethacrylates. The difference in material composition may play an important role in the difference in K_{IC} between the materials tested.(118)

Another likely reason for the differences recorded in K_{IC} may be due to the difference in the polymerization pathway of these materials. The layered, laser-induced polymerization of the P materials is very likely leading to a completely different final structure in these materials. The significant crazing and plastic deformation observed in the 7 d specimens could well be the consequence of the polymerization protocol. Further, spectroscopic, differential scanning calorimetric and dynamic mechanical analyses of the different denture base materials could lead to a better understanding of their structure and properties and may reveal differences in the degree of polymerization and crosslinking between them.

The second null hypothesis (H_{02}) that water storage does not affect the K_{IC} of the denture bases has also been rejected. The results from this study showed that K_{IC} of the C and M denture bases decreased after 90 d of storage in 37 °C. The results of our study are opposite to those by Finoti et al., who reported that K_{IC} of the denture base materials increased after long term water storage.(140) However, the materials tested were not the same. Another study by Wady et. al showed that water has varying effect on the fracture resistance to denture bases.(141) No decrease in the K_{IC} was detected in P denture base group.

Two processes could explain the decrease in K_{IC} upon storage in water: water sorption/desorption and release of residual monomer. Water sorption/desorption is a time dependent process that could have a profound effect on the K_{IC} of denture bases. Water molecules could lead to the displacement of polymer chains, the reduction in intermolecular forces and secondary bonds between the acrylate groups, thereby increasing crack propagation and decreasing K_{IC} .(142)(143) A study by Balkenhol *et al.* has shown that methacrylate-based materials have lower mechanical properties due to weakening of the polymer matrix as a result of water sorption.(144) Water also has a plasticizing effect, thereby decreasing the brittleness of the material. The release of residual

monomers can induce changes in the material composition and structure, affecting mechanical properties and, possibly, reducing the ability to withstand crack propagation.

Another process that may have contributed to the decreased K_{IC} of the specimens after water storage is the loss of plasticizer(s) included in the composition to increase flexibility and the ability to absorb higher energy before failure. Over long-term water storage, the release of plasticizer into water can contribute to the decrease in K_{IC} .(140)(143) Since, printed denture base has undergone complete polymerization during the post processing stage, it can be deduced that no release of the monomer or plasticizer occurred in the printed denture group. Therefore, no change in the K_{IC} values were seen in printed denture base group at 7 d and 90 d.

5.2 Could the notchless triangular prism (NTP specimen K_{IC} test be a better alternative to the SENB test currently recommended by ISO for the determination of fracture toughness of denture base materials?

Finally, considering the good correlation of the results obtained in this study with those obtained by using other test procedures, the small sample volume ($\sim 180 \text{ mm}^3$) compared to ISO recommended SENB sample volume of ($\sim 1250 \text{ mm}^3$), reduced surface flaws and the ease of sample fabrication, the NTP specimen K_{IC} test may be a viable alternative to the single edge notched beam (SENB) test currently recommended by ISO for the determination of K_{IC} of denture base materials.

5.3 Clinical Significance

The results of this study showed that all the tested denture base materials surpassed the 1.9 MPa·m^{1/2} norm set by the International Organization for Standardization (ISO) for K_{IC}.(19) The printed denture base material tested in this study had the highest fracture toughness (~2.2 MPa·m^{1/2}), the highest reliability (m = 24) and the highest work of fracture (~8 KJ/m²), implying a better ability to resist fracture. The longevity of a denture base has a socio-economic impact on the quality of life of the elderly, saving clinical appointment times and millions of dollars in cost.

5.4 Limitations and Future Considerations

The study assessed K_{IC} of a printed denture base printed at 0° plane. Since the printing can be done at varying angulations, such as 45°, 90° etc., we do not know the effect the orientation of the layer/direction of the print has on K_{IC}.

Future spectroscopic, differential scanning calorimetric and dynamic mechanical analyses of the different denture base materials could lead to a better understanding of the property/structure relationship.

Other properties (such as flexural strength, impact strength etc.) need to be investigated.

Only one material was tested for each group. More materials from different manufacturers need to be compared.

Chapter 6: Conclusion

The printed denture base material tested in this study exhibited significantly higher K_{IC} (~ 2.2 MPa \cdot m^{1/2}), absorbed higher energy before fracture (~ 8 KJ/m²) and exhibited stability under ageing conditions, suggesting that it could be more resistant to crack propagation than the conventional and milled materials tested. Of the three test groups, milled denture bases showed least resistance to crack propagation with lowest K_{IC} values both at 7 d and 90 d. Weibull statistics also showed that P group exhibited the highest reliability at 7 d ($m = 24$), followed by C ($m = 19$) and M ($m = 17$) groups. The reliability decreased after 90 d for all groups, with M group exhibiting the lowest reliability ($m = 6$). Water storage for 90 d significantly decreased K_{IC} of C and M groups, with no effect on the K_{IC} of the printed denture bases. Even though the K_{IC} and WOF of P group was higher than that of C and M groups, investigation of the other properties should be done to make informed clinical decision. The results of the study are limited to one material for each group from one manufacturer (Dentsply) and may not be generalized to other denture base materials.

Bibliography

1. Xie Q, Ding T, Yang G. Rehabilitation of oral function with removable dentures - still an option? *J Oral Rehabil.* 2015 Mar;42(3):234–42.
2. McCunniff M, Liu W, Dawson D, Marchini L. Patients' esthetic expectations and satisfaction with complete dentures. *J Prosthet Dent.* 2017 Aug 1;118(2):159–65.
3. Peltzer K, Hewlett S, Yawson A, Moynihan P, Preet R, Wu F, et al. Prevalence of Loss of All Teeth (Edentulism) and Associated Factors in Older Adults in China, Ghana, India, Mexico, Russia and South Africa. *Int J Environ Res Public Health.* 2014 Oct 30;11(11):11308–24.
4. Anusavice KKJK, Phillips RW, Shen C, Rawls HR. *Phillips' science of dental materials.* Elsevier; 2016.
5. Parvizi A, Lindquist T, Schneider R, Williamson D, Boyer D, Dawson D V. Comparison of the dimensional accuracy of injection-molded denture base materials to that of conventional pressure-pack acrylic resin. *J Prosthodont.* 2004 Jun;13(2):83–9.
6. Goodacre BJ, Goodacre CJ, Baba NZ, Kattadiyil MT. Comparison of denture base adaptation between CAD-CAM and conventional fabrication techniques. *J Prosthet Dent.* 2016 Aug 1;116(2):249–56.
7. Duret F, Blouin JL, Duret B. CAD-CAM in dentistry. *J Am Dent Assoc.* 1988;117(6):715–20.
8. Janeva NM, Kovacevska G, Elencevski S, Panchevska S, Mijoska A, Lazarevska B. Advantages of cad/cam versus conventional complete dentures-a review. *Maced J Med Sci.* 2018 Aug 20;6(8):1498–502.

9. Baba NZ, AlRumaih HS, Goodacre BJ, Goodacre CJ. Current techniques in CAD/CAM denture fabrication. *Gen Dent.* 64(6):23–8.
10. Hagman HC. The history of dentures, Part III . *Dent lab Rev.* 1979;54(5):24–5.
11. Kumar MV, Bhagath S, Jei JB. Historical interest of denture base materials. *SRM J Res.* 2010;1(1):103–5.
12. Ladha K, Verma M. 19th century denture base materials revisited. *J Hist Dent.* 2011 Mar;59(1):1–11.
13. Murray MD, Darvell BW. The evolution of the complete denture base. Theories of complete denture retention — A review. Part 1. *Aust Dent J.* 1993;38(3):216–9.
14. Price CA. A history of dental polymers. *Aust Prosthodont J.* 1994;8:47–54.
15. Zarb GA., Bolender CL., Hickey JC, Carlsson GE. *Prosthodontics treatment for edentulous patients.* 13th ed. Mosby, St. Louis;
16. O'Brien W.J. *Dental Materials and Their Selection.* 4th ed. *Journal of Prosthodontics: Implant, Esthetic, and Reconstructive Dentistry.* Quintessence Pub Co; 2009.
17. Maeda Y, Minoura M, Tsutsumi S, Okada M, Nokubi T. A CAD/CAM system for removable denture. Part I: Fabrication of complete dentures. *Int J Prosthodont.* 7(1):17–21.
18. Takahashi Y, Hamanaka I, Shimizu H. Flexural properties of denture base resins subjected to long-Term water immersion. *Acta Odontol Scand.* 2013 May;71(3–4):716–20.
19. ISO - ISO 20795-1:2013 - Dentistry — Base polymers — Part 1: Denture base polymers.

20. Swaney AC, Paffenbarger GC, Caul HJ, Sweeney WT. American Dental Association specification No. 12 for denture base resin: second revision. *J Am Dent Assoc.* 1953 Jan 1;46(1):54–66.
21. Deb S. Polymers in dentistry. *Proc Inst Mech Eng Part H J Eng Med.* 1998 Jun 1;212(6):453–64.
22. Sakaguchi RL., Powers JM. *Craig's Restorative Dental Materials.* Philadelphia, PA, USA: Elsevier/Mosby; 2012.
23. Hassan M., Asghar M., Din SU., Zafar MS. Thermoset Polymethacrylate-Based Materials for Dental Applications; Elsevier: Amsterdam, The Netherlands. 2019. 273–308 p.
24. Manley TR, Bowman AJ, Cook M. Denture bases reinforced with carbon fibres. *Br Dent J.* 1979 Jan;146(1):25–25.
25. Al-Thobity AM. The Impact of Polymerization Technique and Glass-Fiber Reinforcement on the Flexural Properties of Denture Base Resin Material. *Eur J Dent.* 2020 Feb 1;14(1):92–9.
26. Malcom PS. *Polymer Chemistry: An Introduction.* 3rd ed.; Oxford University Press: NY.
27. Demir MM, Memesa M, Castignolles P, Wegner G. PMMA/zinc oxide nanocomposites prepared by in-situ bulk polymerization. *Macromol Rapid Commun.* 2006 May 19;27(10):763–70.
28. Shi M., Kretlow J.D., Spicer PP., et al. Antibiotic-releasing porous polymethylmethacrylate/gelatin/antibiotic constructs for craniofacial tissue engineering. *J Control Release.* 2011;152(1):196–205.
29. Van Krevelen D; NKT. *Properties of polymers.* Elsevier Sciences Publishers, Amsterdam. Wiley; 2000.

30. Alla R., Raghavendra K., Vyas R., Kinakanchi A. Conventional and contemporary polymers for the fabrication of denture prosthesis: Part I—overview, composition and properties. *Int J Appl Dent Sci.* 2015;1(4):82–9.
31. Ogle RE, Sorensen SE, Lewis EA. A new visible light-cured resin system applied to removable prosthodontics. *J Prosthet Dent.* 1986;56(4):497–506.
32. Zafar MS. Prosthodontic applications of polymethyl methacrylate (PMMA): An update. Vol. 12, *Polymers.* MDPI AG; 2020. p. 1–35.
33. Sagsoz NP, Yanıkoglu N, Ulu H, Bayındır F. Color Changes of Polyamid and Polymethyl Methacrylate Denture Base Materials. *Open J Stomatol.* 2014 Oct 24;04(10):489–96.
34. Hada T, Kanazawa M, Iwaki M, Katheng A, Minakuchi S. Comparison of Mechanical Properties of PMMA Disks for Digitally Designed Dentures. *Polymers (Basel).* 2021 May 26;13(11):1745.
35. Lee HH, Lee CJ, Asaoka K. Correlation in the mechanical properties of acrylic denture base resins. *Dent Mater J.* 2012 Jan 21;31(1):157–64.
36. Neihart TR, Li SH, Flinton RJ. Measuring fracture toughness of high-impact poly(methyl methacrylate) with the short rod method. *J Prosthet Dent.* 1988;60(2):249–53.
37. Zafar MS. Wear behavior of various dental restorative materials. *Mater Technol.* 2019 Jan 2;34(1):25–31.
38. Jorge JH, Giampaolo ET, Machado AL, Vergani CE. Cytotoxicity of denture base acrylic resins: A literature review. Vol. 90, *Journal of Prosthetic Dentistry.* Mosby Inc.; 2003. p. 190–3.
39. Lung CYK, Darvell BW. Minimization of the inevitable residual monomer in denture base acrylic. *Dent Mater.* 2005 Dec;21(12):1119–28.

40. Pryor WJ. Injection Molding of Plastics for Dentures. *J Am Dent Assoc.* 1942 Aug 1;29(11):1400–8.
41. Clements JL, Tantbirojn D, Versluis A, Cagna DR. Do denture processing techniques affect the mechanical properties of denture teeth? *J Prosthet Dent.* 2018 Aug 1;120(2):246–51.
42. Nogueira SS, Ogle RE, Davis EL. Comparison of accuracy between compression- and injection-molded complete dentures. *J Prosthet Dent.* 1999;82(3):291–300.
43. Ghazali S El, Glantz PO, Randow K. On the clinical deformation of maxillary complete dentures: Influence of the processing techniques of acrylate-based polymers. *Acta Odontol Scand.* 1988;46(5):287–95.
44. Takamata T, Setcos JC. Resin denture bases: review of accuracy and methods of polymerization. *Int J Prosthodont.* 1989;2(6):555–62.
45. Jackson AD, Lang BR, Wang RF. The influence of teeth on denture base processing accuracy. *Int J Prosthodont.* 1993;6(4):333–40.
46. Woelfel JB, Paffenbarger GC, Sweeney WT. Dimensional changes occurring in dentures during processing. *J Am Dent Assoc.* 1960;61(4):413–30.
47. Gharechahi J., Asadzadeh N., Shahabian F., Gharechahi M. Dimensional changes of acrylic resin denture bases: conventional versus injection-molding technique. *J Dent(Tehran).* 2014;11(4):398–405.
48. Rekow ED, Erdman AG, Riley DR, Klamecki B. CAD/CAM for Dental Restorations—Some of the Curious Challenges. *IEEE Trans Biomed Eng.* 1991;38(4):314–8.
49. Beuer F, Schweiger J, Edelhoff D. Digital dentistry: An overview of recent developments for CAD/CAM generated restorations. *Br Dent J.* 2008 May 10;204(9):505–11.

50. Kanazawa M, Inokoshi M, Minakuchi S, Ohbayashi N. Trial of a CAD/CAM system for fabricating complete dentures. *Dent Mater J*. 2011;30(1):93–6.
51. Soeda Y, Kanazawa M, Arakida T, Iwaki M, Minakuchi S. CAD-CAM milled complete dentures with custom disks and prefabricated artificial teeth: A dental technique. *J Prosthet Dent*. 2020 Nov 12;
52. Baba NZ. Materials and Processes for CAD/CAM Complete Denture Fabrication. *Curr Oral Heal Reports*. 2016 Sep;3(3):203–8.
53. Jain R, Bindra S, Gupta K, Student P. Recent Trends of 3-D Printing in Dentistry-A review. *Ann Prosthodont Restor Dent*. 2(4):101–4.
54. Liu Q, Leu MC, Schmitt SM. Rapid prototyping in dentistry: Technology and application. *Int J Adv Manuf Technol*. 2006 Jun;29(3–4):317–35.
55. Torabi K, Farjood E, Hamedani S. Rapid Prototyping Technologies and their Applications in Prosthodontics, a Review of Literature. Vol. 16, *J Dent Shiraz Univ Med Sci*. 2015.
56. Hull CW, Arcadia C. United States Patent (19) Hull (54) (75) (73) 21) 22 (51) 52) (58) (56) Apparatus for Production of Three-Dimensional Objects by Stereolithography. 1984 Aug.
57. Bibb R, Eggbeer D, Williams R. Rapid manufacture of removable partial denture frameworks. *Rapid Prototyp J*. 2006;12(2):95–9.
58. Hwang HJ, Lee SJ, Park EJ, Yoon HI. Assessment of the trueness and tissue surface adaptation of CAD-CAM maxillary denture bases manufactured using digital light processing. *J Prosthet Dent*. 2019 Jan 1;121(1):110–7.
59. Fueki K, Yoshida E, Igarashi Y. A structural equation model relating objective and subjective masticatory function and oral health-related quality of life in patients with removable partial dentures. *J Oral Rehabil*. 2011 Feb;38(2):86–94.

60. Darvell BW, Clark RKF. The physical mechanisms of complete denture retention. *Br Dent J.* 2000 Sep;189(5):248–52.
61. Sykora O, Sutow EJ. Posterior palatal seal adaptation: influence of processing technique, palate shape and immersion. *J Oral Rehabil.* 1993;20(1):19–31.
62. Steinmassl O, Dumfahrt H, Grunert I, Steinmassl P-A. CAD/CAM produces dentures with improved fit. *Clin Oral Investig.* 2018 Nov 1;22(8):2829–35.
63. Kattadiyil MT, Goodacre CJ, Baba NZ. CAD/CAM complete dentures: a review of two commercial fabrication systems. *J Calif Dent Assoc.* 2013;41(6):407–16.
64. AlHelal A, AlRumaih HS, Kattadiyil MT, Baba NZ, Goodacre CJ. Comparison of retention between maxillary milled and conventional denture bases: A clinical study. *J Prosthet Dent.* 2017 Feb 1;117(2):233–8.
65. Chen H, Wang H, Lv P, Wang Y, Sun Y. Quantitative Evaluation of Tissue Surface Adaption of CAD-Designed and 3D Printed Wax Pattern of Maxillary Complete Denture. *Biomed Res Int.* 2015;2015:453968.
66. Wills DJ, Manderson RD. Biomechanical aspects of the support of partial dentures. *J Dent.* 1977;5(4):310–8.
67. Kawara M, Komiyama O, Kimoto S, Kobayashi N, Kobayashi K, Nemoto K. Distortion behavior of heat-activated acrylic denture-base resin in conventional and long, low-temperature processing methods. *J Dent Res.* 1998;77(6):1446–53.
68. Laughlin GA, Eick JD, Glaros AG, Young L, Moore DJ. A comparison of palatal adaptation in acrylic resin denture bases using conventional and anchored polymerization techniques. Vol. 10, *Journal of Prosthodontics.* 2001. p. 204–11.

69. Nelson MW, Kotwal KR, Sevedge SR. Changes in vertical dimension of occlusion in conventional and microwave processing of complete dentures. *J Prosthet Dent.* 1991;65(2):306–8.
70. Tasaka A, Matsunaga S, Odaka K, Ishizaki K, Ueda T, Abe S, et al. Accuracy and retention of denture base fabricated by heat curing and additive manufacturing. *J Prosthodont Res.* 2019 Jan 1;63(1):85–9.
71. McLaughlin JB, Ramos V, Dickinson DP. Comparison of Fit of Dentures Fabricated by Traditional Techniques Versus CAD/CAM Technology. *J Prosthodont.* 2019 Apr 1;28(4):428–35.
72. Lee S, Hong SJ, Paek J, Pae A, Kwon KR, Noh K. Comparing accuracy of denture bases fabricated by injection molding, CAD/CAM milling, and rapid prototyping method. *J Adv Prosthodont.* 2019;11(1):55–64.
73. Alghazzawi TF. Advancements in CAD/CAM technology: Options for practical implementation. Vol. 60, *Journal of Prosthodontic Research.* Elsevier Ltd; 2016. p. 72–84.
74. Steinmassl PA, Wiedemair V, Huck C, Klaunzer F, Steinmassl O, Grunert I, et al. Do CAD/CAM dentures really release less monomer than conventional dentures? *Clin Oral Investig.* 2017 Jun 1;21(5):1697–705.
75. Rashid H, Sheikh Z, Vohra F. Allergic effects of the residual monomer used in denture base acrylic resins. Vol. 9, *European Journal of Dentistry.* Dental Investigations Society; 2015. p. 614–9.
76. Lung CYK, Darvell BW. Minimization of the inevitable residual monomer in denture base acrylic. *Dent Mater.* 2005 Dec 22;21(12):1119–28.

77. Bartoloni JA, Murchison DF, Wofford DT, Sarkar NK. Degree of conversion in denture base materials for varied polymerization techniques. *J Oral Rehabil.* 2000;27(6):488–93.
78. Vallittu PK, Miettinen V, Alakuijala P. Residual monomer content and its release into water from denture base materials. *Dent Mater.* 1995;11(5–6):338–42.
79. Infante L, Yilmaz B, McGlumphy E, Finger I. Fabricating complete dentures with CAD/CAM technology. *J Prosthet Dent.* 2014;111(5):351–5.
80. Murakami N, Wakabayashi N, Matsushima R, Kishida A, Igarashi Y. Effect of high-pressure polymerization on mechanical properties of PMMA denture base resin. *J Mech Behav Biomed Mater.* 2013 Apr;20:98–104.
81. Prpić V, Schauerl Z, Čatić A, Dulčić N, Čimić S. Comparison of Mechanical Properties of 3D-Printed, CAD/CAM, and Conventional Denture Base Materials. *J Prosthodont.* 2020 Apr 20;jopr.13175.
82. Ashby MF, Shercliff H., Cebon D. *Materials Selection in Mechanical Design* (3rd ed.). Burlington, Massachusetts: Butterworth-Heinemann. 1999.
83. Srinivasan M, Gjengedal H, Cattani-Lorente M, Moussa M, Durual S, Schimmel M, et al. CAD/CAM milled complete removable dental prostheses: An in vitro evaluation of biocompatibility, mechanical properties, and surface roughness. *Dent Mater J.* 2018;37(4):526–33.
84. Al-Dwairi ZN, Tahboub KY, Baba NZ, Goodacre CJ. A Comparison of the Flexural and Impact Strengths and Flexural Modulus of CAD/CAM and Conventional Heat-Cured Polymethyl Methacrylate (PMMA). *J Prosthodont.* 2020 Apr;29(4):341–9.
85. Ayman A-D. The residual monomer content and mechanical properties of CAD\CAM resins used in the fabrication of complete dentures as compared to heat cured resins. *Electron Physician.* 2017 Jul 25;9(7):4766–72.

86. Sepúlveda-Navarro WF, Arana-Correa BE, Ferreira Borges CP, Habib Jorge J, Urban VM, Campanha NH. Color stability of resins and nylon as denture base material in beverages. *J Prosthodont*. 2011 Dec;20(8):632–8.
87. Arana-Correa BE, Sepúlveda-Navarro WF, Florez FL, Urban VM, Jorge JH, Campanha NH. Colour stability of acrylic resin denture teeth after immersion in different beverages. *Eur J Prosthodont Restor Dent*. 2014;22(2):56–61.
88. Goiato MC, dos Santos DM, Haddad MF, Pesqueira AA. Effect of accelerated aging on the microhardness and color stability of flexible resins for dentures. *Braz Oral Res*. 2010 Jan;24(1):114–9.
89. Goiato MC, Nóbrega AS, dos Santos DM, Andreotti AM, Moreno A. Effect of different solutions on color stability of acrylic resin-based dentures. *Braz Oral Res*. 2014;28(1).
90. Omata Y, Uno S, Nakaoki Y, Tanaka T, Sano H, Yoshida S, et al. Staining of hybrid composites with coffee, oolong tea, or red wine. *Dent Mater J*. 2006 Mar;25(1):125–31.
91. Ceci M, Viola M, Rattalino D, Beltrami R, Colombo M, Poggio C. Discoloration of different esthetic restorative materials: A spectrophotometric evaluation. *Eur J Dent*. 2017;11(2):149–56.
92. Alt V, Hannig M, Wöstmann B, Balkenhol M. Fracture strength of temporary fixed partial dentures: CAD/CAM versus directly fabricated restorations. *Dent Mater*. 2011 Apr;27(4):339–47.
93. Stawarczyk B, Ender A, Trottmann A, Özcan M, Fischer J, Hämmerle CHF. Load-bearing capacity of CAD/CAM milled polymeric three-unit fixed dental prostheses: Effect of aging regimens. *Clin Oral Investig*. 2012 Dec;16(6):1669–77.

94. Dayan C, Guven M, Gencel B, Bural C. A Comparison of the Color Stability of Conventional and CAD/CAM Polymethyl Methacrylate Denture Base Materials. *Acta Stomatol Croat.* 2019;53(2).
95. AlQarni FD, Goodacre CJ, Kattadiyil MT, Baba NZ, Paravina RD. Stainability of acrylic resin materials used in CAD-CAM and conventional complete dentures. *J Prosthet Dent.* 2019 Nov 5;
96. Saponaro PC, Yilmaz B, Heshmati RH, McGlumphy EA. Clinical performance of CAD-CAM-fabricated complete dentures: A cross-sectional study. *J Prosthet Dent.* 2016 Sep 1;116(3):431–5.
97. Kattadiyil MT, Jekki R, Goodacre CJ, Baba NZ. Comparison of treatment outcomes in digital and conventional complete removable dental prosthesis fabrications in a predoctoral setting. *J Prosthet Dent.* 2015 Dec 1;114(6):818–25.
98. Bidra AS, Farrell K, Burnham D, Dhingra A, Taylor TD, Kuo CL. Prospective cohort pilot study of 2-visit CAD/CAM monolithic complete dentures and implant-retained overdentures: Clinical and patient-centered outcomes. *J Prosthet Dent.* 2016 May 1;115(5):578-586.e1.
99. Drago C, Borgert AJ. Comparison of nonscheduled, postinsertion adjustment visits for complete dentures fabricated with conventional and CAD-CAM protocols: A clinical study. *J Prosthet Dent.* 2019 Nov 1;122(5):459–66.
100. Srinivasan M, Schimmel M, Naharro M, O' Neill C, McKenna G, Müller F. CAD/CAM milled removable complete dentures: time and cost estimation study. *J Dent.* 2019 Jan 1;80:75–9.

101. Kalberer N, Mehl A, Schimmel M, Müller F, Srinivasan M. CAD-CAM milled versus rapidly prototyped (3D-printed) complete dentures: An in vitro evaluation of trueness. *J Prosthet Dent.* 2019 Apr 1;121(4):637–43.
102. Coco BJ, Bagg J, Cross LJ, Jose A, Cross J, Ramage G. Mixed *Candida albicans* and *Candida glabrata* populations associated with the pathogenesis of denture stomatitis. *Oral Microbiol Immunol.* 2008 Oct;23(5):377–83.
103. Ramage G, Martínez JP, López-Ribot JL. *Candida* biofilms on implanted biomaterials: A clinically significant problem. In: *FEMS Yeast Research.* 2006. p. 979–86.
104. Wolfaardt JF, Cleaton-Jones P, Fatti P. The occurrence of porosity in a heat-cured poly (methyl methacrylate) denture base resin. *J Prosthet Dent.* 1986;55(3):393–400.
105. Radford DR, Sweet SP, Challacombe SJ, Walter JD. Adherence of *Candida albicans* to denture-base materials with different surface finishes. *J Dent.* 1998;26(7):577–83.
106. Al-Fouzan AF, Al-Mejrad LA, Albarrag AM. Adherence of *Candida* to complete denture surfaces in vitro: A comparison of conventional and CAD/CAM complete dentures. *J Adv Prosthodont.* 2017 Oct 1;9(5):402–8.
107. Verhaeghe T V., Wyatt CC, Mostafa NZ. The effect of overnight storage conditions on complete denture colonization by *Candida albicans* and dimensional stability: A systematic review. *Journal of Prosthetic Dentistry.* Mosby Inc.; 2019.
108. Miettinen VM, Vallittu PK. Water sorption and solubility of glass fiber-reinforced denture polymethyl methacrylate resin. *J Prosthet Dent.* 1997 May 1;77(5):531–4.
109. Stephens A.P. Midline fracture of complete dentures. *Mississippi Dent Assoc J.* 1979;35(3):28–9.

110. Kim SH, Watts DC. The effect of reinforcement with woven E-glass fibers on the impact strength of complete dentures fabricated with high-impact acrylic resin. *J Prosthet Dent.* 2004 Mar;91(3):274–80.
111. Hargreaves AS. The prevalence of fractured dentures. A survey. *Br Dent J.* 1969;126(10):451–5.
112. Beyli MS, von Fraunhofer JA. An analysis of causes of fracture of acrylic resin dentures. *J Prosthet Dent.* 1981;46(3):238–41.
113. Kelly E. Fatigue failure in denture base polymers. *J Prosthet Dent.* 1969;21(3):257–66.
114. Rees J, Huggett R, Harrison A. Finite element analysis of the stress-concentrating effect of fraenal notches in complete dentures. *Int J Prosthodont.* 1990;3(3):238–40.
115. Nejatidanesh F, Peimannia E, Savabi O. Effect of labial frenum notch size and palatal vault depth on stress concentration in a maxillary complete denture: a finite element study. *J Contemp Dent Pr.* 2009;10(3):59–66.
116. Cilingir A, Bilhan H, Baysal G, Sunbuloglu E, Bozdog E. The impact of frenulum height on strains in maxillary denture bases. *J Adv Prosthodont.* 2013;409:409–24.
117. Mutlu G., Harrison A., Huggett R. A history of denture base materials. 1989;13: 145-51. *Quintessence Dent Technol Yearb.* 1989;13:145–51.
118. Stafford GD, Huggett R, Causton BE. Fracture toughness of denture base acrylics. *J Biomed Mater Res.* 1980;14(4):359–71.
119. Griffith AA. The phenomena of rupture and flow in solids. *Phil. Trans. Roy. Soc. London A* 1920, 221, 163–198.
120. Rodford R. The development of high impact strength denture-base materials. *J Dent.* 1986;14(5):214–7.

121. Collyer AA. Rubber Toughened Engineering Plastics. Rubber Toughened Engineering Plastics. Springer Netherlands; 1994.
122. Dowling NE. Mechanical behavior of materials: engineering methods for deformation, fracture, and fatigue. 4th ed. Pearson Education Limited; 2013.
123. Barker LM. A simplified method for measuring plane strain fracture toughness. Eng Fract Mech. 1977 Jan 1;9(2):361–9.
124. Mostovoy S, Rippling EJ. Fracture toughness of an epoxy system. J Appl Polym Sci. 1966 Sep 1;10(9):1351–71.
125. ASTM D5045 - 99(2007)e1 Standard Test Methods for Plane-Strain Fracture Toughness and Strain Energy Release Rate of Plastic Materials.
126. Ruse ND, Troczynski T, MacEntee MI, Feduik D. Novel fracture toughness test using a notchless triangular prism (NTP) specimen. J Biomed Mater Res. 1996 Aug 1;31(4):457–63.
127. Zappini G, Kammann A, Wachter W. Comparison of fracture tests of denture base materials. J Prosthet Dent. 2003;90(6):578–85.
128. Ruse ND. Fracture mechanics characterization of dental biomaterials. In: Dental Biomaterials: Imaging, Testing and Modelling. Elsevier Inc.; 2008. p. 261–93.
129. Alkadi L, Ruse ND. Fracture toughness of two lithium disilicate dental glass ceramics. In: Journal of Prosthetic Dentistry. Mosby Inc.; 2016. p. 591–6.
130. Berry JP. Fracture processes in polymeric materials. II. The tensile strength of polystyrene. J Polym Sci. 1961 Apr 1;50(154):313–21.
131. van Belle G. Statistical Rules of Thumb: Second Edition. Statistical Rules of Thumb: Second Edition. wiley; 2008.

132. Kusy RP, Lytwyn BJ, Turner DT. Characterization of Cross-Linked Two-Phase Acrylic Polymers. *J Dent Res.* 1976 May 9;55(3):452–9.
133. Hargreaves AS. The effect of the environment on the crack initiation toughness of dental poly(methyl methacrylate). *J Biomed Mater Res.* 1981 Sep 1;15(5):757–68.
134. Pilliar RM, Vowles R, Williams DF. Fracture toughness testing of biomaterials using a mini-short rod specimen design. *J Biomed Mater Res.* 1987;21(1):145–54.
135. Soderholm KJ. Review of the fracture toughness approach. Vol. 26, *Dental Materials.* Dent Mater; 2010.
136. Quinn GD, Quinn JB, Quinn GD. A practical and systematic review of Weibull statistics for reporting strengths of dental materials. *Dental Materials Dent Mater;* Feb p. 135–47.
137. Bubsey RT, Munz D, Pierce WS, Shannon JL. Compliance calibration of the short rod chevron-notch specimen for fracture toughness testing of brittle materials. *Int J Fract.* 1982 Feb;18(2):125–33.
138. Pacquet W, Benoit A, Hatège-Kimana C, Wulfman C. Mechanical Properties of CAD/CAM Denture Base Resins. *Int J Prosthodont.* 2018 Jan;32(1):104–6.
139. D B. *Elementary engineering fracture mechanics.* 1986;4. Boston, Kluwer Academic Publishers.
140. Finoti LS, MacHado AL, Chaves CDAL, Pavarina AC, Vergani CE. Effect of long-term water immersion on the fracture toughness of denture base and reline resins. *Gerodontology.* 2012 Jun;29(2).
141. Wady AF, Machado AL, Vergani CE, Pavarina AC, Giampaolo ET. Impact strength of denture base and reline acrylic resins subjected to long-term water immersion. *Braz Dent J.* 2011;22(1):56–61.

142. Rantala LI, Lastumäki TM, Peltomäki T, Vallittu PK. Fatigue resistance of removable orthodontic appliance reinforced with glass fibre weave. *J Oral Rehabil.* 2003 May 1;30(5):501–6.
143. Urban VM, Machado AL, Vergani CE, Giampaolo ET, Pavarina AC, de Almeida FG, et al. Effect of water-bath post-polymerization on the mechanical properties, degree of conversion, and leaching of residual compounds of hard chairside reline resins. *Dent Mater.* 2009 May;25(5):662–71.
144. Balkenhol M, Köhler H, Orbach K, Wöstmann B. Fracture toughness of cross-linked and non-cross-linked temporary crown and fixed partial denture materials. *Dent Mater.* 2009 Jul;25(7):917–28.